THERMOPHILIC ANAEROBIC DIGESTION OF WASTEWATER SLUDGE

THERMOPHILIC ANAEROBIC DIGESTION OF WASTEWATER SLUDGE

By: YOUSIF HIRMIZ, B. Eng.

A Thesis Submitted to the School of Graduate Studies in Partial Fulfillment of the Requirements for the Degree

Master of Applied Science

McMaster University

McMaster University MASTER OF APPLIED SCIENCE (2018) Hamilton, Ontario (Civil Engineering)

TITLE: thermophilic anaerobic digestion of wastewater sludge

AUTHOR: Yousif Hirmiz, B. Eng. (McMaster University)

SUPERVISOR: Dr. Younggy Kim

NUMBER OF PAGES: xii, 76

Abstract

Sludge management is the highest operating cost in municipal wastewater treatment. Anaerobic digestion (AD) is used to stabilize the sludge and reduce biosolids generation. Hydrolysis kinetics limit the rate of anaerobic digestion and must be improved to increase the overall process rate. In this study a new sludge characterization analysis was used to evaluate hydrolysis in a lab-scale pretreatment process operated at 55℃, 65℃, and 75℃. The experimental results were used to develop a new AD mathematical model, the hydrolysis digestion model (HDM). The model developed is easier to use, as the number of processes and variables were reduced by half, in comparison to existing models. The model variables can be measured using standard sludge characterization analysis, and the hydrolysis reactions included the fermenting microorganism to more accurately model the two-phase hydrolysis model. Model simulations were found to be a good fit of the experimental results, accurately predicting the rate and extent of hydrolysis in the pretreatment digester.

Acknowledgments

I am blessed to live in a country like Canada, where I have been privileged with the opportunity to pursue a higher level of education. I would like to recognize all the educators, family and friends that have taught and supported me in the years leading up to my master's degree. In completing this thesis, I am indebted to:

My supervisor, Dr. Younggy Kim, for the opportunity to learn, think and grow under your consistent support and supervision. Thank you for teaching me everything I know on wastewater treatment, through the courses you taught and the discussions we had. I appreciate how available you made yourself, and the guidance you provided through every step of this project. I could not have done this without you.

Youngseck Hong, for the continuous support and feedback in helping me improve my work. Thank you for always helping me look at the big picture, for challenging me on the small details, and trusting in my work. Monica Han, for an outstanding job supervising the environmental lab. Thank you for always being available to offer your help and expertise in teaching me new laboratory techniques. Wendy Huang: thank you for helping me get settled into the lab and for sharing your experience with lab scale anaerobic digesters.

My dissertation committee members, Dr. David Latulippe, and Dr. Yiping Guo, for your time and insightful comments in helping me improve my work.

To my parents, Najeeb Hirmiz, and Nadera Oraha, for the sacrifices you have made and continue to make, so that I may continue to have better opportunities in life. **Totus Tuus!**

Table of Contents

List of Figures

List of Tables

List of Abbreviations

AD	Anaerobic Digestion
ADM1	Anaerobic Digestion Model No.1
BMP	Biochemical methane potential
COD	Chemical oxygen demand (g-COD/L)
EPA	Environmental Protection Agency
EPS	Extracellular polymeric substances
FA	Free ammonia (NH_3)
GC	Gas chromatography
GHG	Greenhouse gases
HDM	Hydrolysis digestion model
IS	Inert solids (g-IS/L)
ISS	Inert suspended solids (g-ISS/L)
LCFA	Long chain fatty acid
MAD	Mesophilic anaerobic digestion
RRF	Resource recovery facilities
SCFA	Short chain fatty acid
SCOD	Soluble chemical oxygen demand (g-COD/L)
SRT	Solids retention time (days)
SV	Sensitivity value
TAD	Thermophilic anaerobic digestion
TCOD	Total chemical oxygen demand (g-COD/L)
TS	Total solids (g-TS/L)
TSS	Total suspended solids (g-TSS/L)
TWAS	Thickened waste activated sludge

V	Volume of sludge (L)
VBA	Visual basic application
VS	Volatile solids (g-VS/L)
VSS	Volatile suspended solids (g-VSS/L)
WAS	Waste activated sludge
WWTP	Wastewater treatment plant

Declaration of Academic Achievement

Thesis includes two chapters that are intended for publication. Chapter 2 is intended for publication in a peer-reviewed scientific journal, and chapter 3 is intended to be published as a conference paper. I will be the primary author on both articles, my supervisor Dr. Younggy Kim will be the second author, and Youngseck Hong will be the third author. My contributions to the work include literature review, conducting experiments, data analysis, mathematical model development, and manuscript writing. My supervisor provided guidance, support, training, and expertise during every stage of the work. The third author provided support, and guidance on the direction of the work and the interpretation of results.

1 Introduction

1.1 Anaerobic digestion

Sludge is a by-product of the conventional waste activated sludge (WAS) process for treating municipal wastewater. Two types of sludge are generated; primary sludge composed of particulate organics and WAS composed mainly of microorganisms in polymeric networks (Raszka, Chorvatova, & Wanner, 2006). Transportation of sludge for direct disposal is expensive and often unfeasible given the large volumes of sludge generated. Furthermore, direct landfilling has a negative environmental impact as the organics in the sludge breakdown over time into greenhouse gases: methane and carbon dioxide. Thus, sludge must be reduced and stabilized at the wastewater treatment plant (WWTP) prior to disposal. Sludge management processes reduce the mass and volume of biosolids generated and stabilize the sludge, which reduces degradation in landfills, odours and pathogens (Grady, Daigger, Love, & Filipe, 2011). For most WWTPs, the sludge management and disposal process represent the highest operating cost (Vlyssides & Karlis, 2004)(Neyens, Baeyens, Dewil, & De Heyder, 2004).

In a standard sludge treatment process, the two main objectives are sludge stabilization and water removal (H. Carrère et al., 2010). Water removal using centrifuges, gravity belt thickeners or polymer flocculants allows for sludge thickening, and volume reduction. Thickened sludge is stabilized by incineration, pyrolysis, or anaerobic digestion (AD). AD is the most commonly used method for municipal sludge stabilization (Chen, Cheng, & Creamer, 2008). AD is a slow biological process limited by microbial kinetics;

thus, the solids retention time (SRT) in an anaerobic digester is usually greater than 15 days (Noike, Endo, Chang, Yaguchi, & Matsumoto, 1985) (Toreci, Kennedy, & Droste, 2009). Digesters operating at a long SRT must be large to hold sludge for 15 days. Large digesters are expensive to build and have high operating costs. Heating is the main operating cost and its more significant in colder climates.

In recent years both academia and industry have invested energy, time and money to improve the AD process. Several factors are driving this need to improve AD including; the banning of other sludge stabilization processes and the attempt to transform WWTP into resource recovery facilities. Quebec and other Canadian provinces will ban the incineration and landfilling of biosolids from wastewater treatment facilities starting 2022, in an effort to reduce greenhouse gas emissions (Langlois, 2017). Plants currently using incineration will likely switch to AD. At the same time, the wastewater treatment community is looking to convert WWTPs to resource recovery facilities (RRF). AD fits the theme of RRF as it can generate biogas for energy; moreover, given the proper sludge reduction and pathogen inactivation, the biosolids generated at the end of the process can be used for agricultural land application. Thus, there is an economical, environmental and social incentive to reduce the overall process SRT, increase biogas generation and increase solids reduction.

1.2 Literature review: biological reactions in anaerobic digestion

Anaerobic digestion is the process of stabilizing sludge, by reducing insoluble organics to biogas (Grady et al., 2011). Biogas is made up of 70 % methane and 30 %

carbon dioxide (Werker, Carlsson, Morgan-Sagastume, Le, & Harrison, 2007) (Rea, 2014). Plants use biogas as fuel to heat up anaerobic digesters or convert it to electricity. The first step in the anaerobic digestion process is the hydrolysis of particulate organics into soluble substrate. It is followed by acidogenesis where soluble substrate is converted to hydrogen gas, and short chain fatty acids (SCFA). Short chain fatty acids are reduced further to acetic acid through the third step of acetogenesis. In the final step, hydrogen gas, and acetic acid are converted to methane in a process known as methanogenesis. All reactions are carried forward by microorganisms and take place both in series and in parallel.

In municipal WWTPs, the sludge from both primary and secondary clarifiers is composed of particulate organics. WAS from secondary clarifiers is difficult to breakdown. The organic content of WAS is mainly biomass, clustered in a polymeric network which allows the biomass to form flocs and settle out in secondary clarifiers (Tenney & Stumm, 1965). The polymeric network formed by filamentous bacteria is made up of extracellular polymeric substances, which are composed mainly of proteins and polysaccharides (Wanner, 1994) (Raszka et al., 2006). Polymeric networks retain water, which allows them to build up the nutrient concentration necessary for bacteria to flourish (Grady et al., 2011). The network also protects the microorganisms, acting as a barrier to toxins (Raszka et al., 2006). Disintegration of the polymer network is important for both dewatering of sludge and for accessing the organics in WAS (Keiding, Wybrandt, & Nielsen, 2001). The accessibility of microorganisms to the biodegradable organics in WAS is the limiting factor in anaerobic digestion.

Cell lysis produces biodegradable organics and inert inorganic material(Batstone et al., 2002). Particulate organics are broken down to macromolecules: lipids, proteins and carbohydrates. The macromolecules are hydrolyzed into their monomer units by extracellular enzymes. Literature suggests two models for hydrolysis reactions; in the first model, extracellular enzymes produced by fermenters in the digester are released into a suspension of particulate organics. The organics that react with the hydrolytic enzymes are broken down (Vavilin, Rytov, & Lokshina, 1996). The second model is the two-phase model, where in the first phase, fermenters colonize the surface of the particulate organics and release enzymes within its vicinity (Vavilin et al., 1996). In the second phase, the fermenters use the hydrolysed substrate to grow, and form new daughter cells that fall off and colonize a new surface.

Hydrolysis is a reaction that aims to reduce the size of macromolecules. Hydrolysis of carbohydrates to soluble sugars and proteins to amino acids is relatively rapid (1-3 days) (Grady et al., 2011). Hydrolysis of lipids to long chain fatty acids (LCFAs) is slower (4 to 6 days) (Grady et al., 2011). The soluble chemical oxygen demand (SCOD), and the volatile suspended solids (VSS) are good indicators of hydrolysis reactions and solubilization of organics. The chemical oxygen demand (COD), a measure of pollutant strength, is an indicator of the concentration of electrons, in g-COD/L. In wastewater treatment, it is a standard method of characterizing sludge and determining its organic content, by reporting the amount of oxygen required to oxidize the organics in the sludge (Grady et al., 2011). The fraction of organics in sludge that can be taken up as substrate by microorganisms, is referred to as the SCOD. Standard methods defines SCOD as the fraction of organics that

is not filterable by a filter with a pore size of 2 μm; while the VSS are the fraction of organics that are filtered out by a filter with a pore size of 2 μm and volatilized at 505℃ (APHA/AWWA/WEF, 2012). During hydrolysis reactions the VSS are reduced while the SCOD increases.

The products of the hydrolysis reactions are the substrates for the acidogenesis reactions. Under anaerobic conditions, fermenters convert sugars, and amino acids to carbon dioxide, hydrogen gas and short chain fatty acids (SCFAs). In this reaction, the substrate is both the electron acceptor and the electron donor. This process is fast < 1 day, and robust as the community of fermentative bacteria is diverse (Grady et al., 2011). The fermentation of LCFAs is done through a cyclic process known as β – oxidation. One molecule of acetate is removed per a cycle; the products of each cycle are acetic acid, carbon dioxide and H^+ ions (Madigan, 2014). β – oxidation is also used to convert SCFAs, including butyric acid, and propanoic acid to acetic acid. Hydrogen gas plays an important role in the anaerobic digestion process as the electron sink in the digester. Its concentration must be kept at a minimum in the digester because at standard conditions, the Gibbs free energy of the β – oxidation reaction is positive, and thus the reaction will not proceed spontaneously. Hydrogen ions exit the digester in the gas form as H_2 gas or are used up by hydrogenotrophic methanogens to generate methane gas. Maintaining the concentration of soluble hydrogen gas at a minimum results in a negative Gibbs free energy and drives the β – oxidation reaction forward (Grady et al., 2011). The relationship between β –oxidizers and hydrogenotrophic methanogens is know as obligate syntrophy; both microorganisms need and benefit from each other to complete their biochemical reactions (Madigan, 2014).

Without the hydrogenotrophic methanogens, AD would stop at the fermentation of sugars and amino acids. With most of the electrons in the anaerobic oxidation reaction transferred to hydrogen gas, the biomass growth yield is very small and thus require ~ 4 to 6 days for the microbial community to grow to a level where it can actively convert the LCFAs and SCFAs to methanogenic substrates (Grady et al., 2011).

Acetic acid, carbon dioxide and the hydrogen gas produced via the acidogenesis and acetogenesis reactions are used as substrates for methanogenesis. Hydrogenotrophic methanogens use hydrogen gas as the electron donor to reduce carbon dioxide and form methane gas. The reaction is fast (1 to 2 days), and robust as the microbial community is made up of a diverse group of *Archea* species that rapidly grow to sufficient populations (Grady et al., 2011). The second type of methanogens found in anaerobic digesters convert acetic acid into methane and carbon dioxide. In this reaction, the acetic acid is both the electron donor and acceptor. Acetoclastic methanogens are not diverse, and as a result the overall reaction is slow, and often inhibited by environmental conditions (Grady et al., 2011). The two-main species found are *Methanosarcina* spp. and *Methanosaeta* spp. The first is a copiotroph, and favours an environment with a high acetic acid concentration (Madigan, 2014). *Methanosarcina* spp. grow rapidly, 3 to 5 days (Grady et al., 2011). Municipal anaerobic digesters are operated at steady state and the concentration of acetic acid is kept low; thus, *Methanosaeta* spp. which are oligotrophs and prefer a low acetic acid concentration for growth are more dominant. *Methanosaeta* spp. are slow and require 12 to 15 days to grow (Grady et al., 2011). Acetoclastic methanogens are sensitive to their environment-pH, free ammonia concentration, and temperature are all factors that must be

kept within a specific range. Inhibition of the reaction by deviations from the operating range of the acetoclastic methanogens often results in digester instability.

1.3 Literature review: thermophilic anaerobic digestion

Cell lysis and hydrolysis of particulate organics are the rate limiting reactions in anaerobic digestion. Most anaerobic digesters are operated at mesophilic temperatures. Mesophilic anaerobic digestion (MAD) is more stable, and has a lower energy requirement, in comparison to thermophilic anaerobic digestion (TAD) (Nosrati, Amani, & Sreekrishnan, 2011). Operating at higher temperatures increases hydrolytic activity, and microorganism growth rate; thus, the overall solids destruction rate increases (Ariunbaatar, Panico, Esposito, Pirozzi, & Lens, 2014). A more rapid solids reduction rate does not increase the extent of biodegradability, but lowers the overall SRT. The advantages to operating at a shorter SRT include a higher digestion capacity, smaller digester size, and reduced mixing requirements (Labatut, Angenent, & Scott, 2014). Digestion at higher temperatures increases the heating requirements; however, a shorter SRT reduces the heating requirement time and increases the biogas generation rate. New plants may choose to operate at thermophilic conditions to reduce the initial capital cost, while existing plants may choose to operate under thermophilic conditions to increase digester capacity.

The two main reasons for lower stability in TAD are a less diverse microbial community and accumulation of inhibitory substances. The microbial community is less diverse at higher temperatures; thus, the active microorganisms are more sensitive to the environment (Labatut et al., 2014). Temperature increase impacts the various biochemical process differently. This often leads to the accumulation of intermediate reactants, which

can cause process inhibition. In the digester, ammonia accumulation occurs at higher protein hydrolysis rates. Ammonia has two main forms: ammonium ion NH_4^+, and free ammonia (FA) NH_3. FA is membrane permeable, and once inside the cell it disrupts the homeostatic equilibrium of microorganisms (Chen et al., 2008). The less diverse acetoclastic methanogens are impacted the most by FA, as the homeostatic imbalance inhibits cell growth. Inhibited methanogenesis results in lower methane production and the accumulation of acetic acid (Labatut et al., 2014). The accumulation of acetic acid, and hydrogen gas thermodynamically inhibit the β-oxidation of LCFA and SCFA (Labatut et al., 2014). The accumulation of acetic acid also lowers digester pH, which impacts the growth rate of microorganisms (Chen et al., 2008). Lower pH reduces the FA concentration and converts it to ammonium ion; this allows methanogens to grow and restores digester stability. The overall methane yield is reduced and thus the digester operates at an "inhibited steady-state" (Chen et al., 2008).

1.4 Literature review: sludge pretreatment to enhance anaerobic digestion of WAS

The rate limiting hydrolysis reaction is the first step in AD; thus, it can be isolated and improved outside the digester using sludge pretreatment processes. Pretreatment processes increase the rate of solids destruction; thus, increasing the rate limiting hydrolysis reactions. A great number of pretreatment processes have been studied: including thermal, physical, chemical and biological (Pesante & Vidal, 2016). Choosing a process most suitable depends on the type of sludge, cost of treatment, local regulations on chemical consumption, reliability of the process and safety factors. Studies have shown that pretreatment processes have a greater impact on the degradability of WAS, in comparison

to primary sludge. The impact is also greater when the pretreatment is followed by MAD in comparison to TAD (Pesante & Vidal, 2016) (H. Carrère et al., 2010).

Chemical processes are the least studied category of pretreatment processes, with ozonation being the most studied in this category (Pesante & Vidal, 2016). Ozone O_3 is a very strong oxidizer, that breaks down into radicals that are capable of oxidizing organics (Klein, 2016). The objective in ozone treatment is to oxidize and breakdown the particulate organics without oxidizing the soluble organics. To accomplish this, the dosage of ozone added must be controlled. The optimal dosage is sludge dependant, with various studies reporting a dosage in the range of 0.05 – 0.5 gO_3/gTS (Pesante & Vidal, 2016). Weemaes et al. reported that at an ozone dosage of 0.2 $gO_3/gCOD$, 38 % of the organic matter could be oxidized and 29 % solubilized; while 80 % increase in methane production could be achieved at a dosage of 0.1 $gO_3/gCOD$ (Weemaes, Grootaerd, Simoens, & Verstraete, 2000). Ozone, which is not transported and must be created on site, is used in water treatment processes for disinfection; thus, it can reduce the pathogens in biosolids.Ozone generation is energy demanding and the process must be highly regulated to ensure safety. This is the main disadvantage of using ozone as a pretreatment process.

Thermal pretreatment processes are organized into three categories based on temperature: high-temperature treatment (> 100 ℃), low temperature treatment (<100 ℃), and freezing/ thawing. High-temperature thermal hydrolysis effectively solubilizes sludge, through physical disruption and cell lysis. At high temperatures, solubilization rate is independent of sludge source, while the extent of solubilization is directly linked to process temperature (Hélène Carrère, Bougrier, Castets, & Delgenès, 2008) (Pesante & Vidal,

2016). Bougrier et al. reported that for temperatures below 200 ℃, solubilization linearly increased with increasing temperature (Bougrier, Delgenès, & Carrère, 2008). A temperatures range of 100-200 ℃ is broad and thus different temperatures are better for the solubilization of various sludge fractions. High temperature thermal hydrolysis reduces sludge viscosity, which lowers operating costs associated with pumping and mixing of sludge (Graja, Chauzy, Fernandes, Patria, & Cretenot, 2005). High temperatures eliminate pathogens in the sludge, producing biosolids that can be used as fertilizer. The disadvantage of high temperature thermal hydrolysis is the high energy demand used to heat up sludge to temperatures greater than 100 ℃. However, the extra energy can be reduced or even eliminated by the increase in biogas production. The high increase in protein solubilization leads to high concentrations of ammonia, which can inhibit AD. Temperatures higher than 200 ℃ degrade nitrogenous compounds, and polymerization reactions form undesirable refractory components.

Low-temperature thermal pretreatment processes increase the rate of hydrolysis by using hydrolytic enzymes released from the sludge, active thermophilic bacteria, and thermal solubilization of organics (Carvajal, Peña, & Pérez-Elvira, 2013). At temperatures below 100℃, time and sludge source in addition to temperature, impact solubilization (Nazari et al., 2017). Nazari et al. investigated the relationship between temperature, time and their effect in solubilizing sludge from various sources. In the study he concluded that higher temperatures and longer SRT increased solubilization of organic matter in WAS, in particular proteins (Nazari et al., 2017).

Autohydrolysis is considered a biological pretreatment process, that also falls within the low-temperature thermal pretreatment range. WAS from secondary clarifiers is subject to new environmental conditions including limited oxygen and high temperatures (≥45℃). Microorganisms respond by releasing hydrolytic enzymes which increase the rate of solubilization (Pesante & Vidal, 2016). The clear advantage of this process is reduced costs, both capital and operating. At temperatures lower than 100℃, the energy demand for this process is significantly smaller than that for high-temperature thermal hydrolysis. Chemical use is not required as the process exploits the hydrolytic potential of WAS. Specific equipment such as that used in ultrasound, or ozonation is not required. At lower temperatures this process can not fully remove pathogens.

Carvajal et al. studied the effect of varying sludge concentrations, and oxygen supply in a autohydrolysis pretreatment processes, using lab scale (Carvajal et al., 2013). In the study, sludge at concentrations of 23 and 54 Kg $m^{-3}$of TS was treated for a day, at a temperature of 55℃, under anaerobic conditions (Carvajal et al., 2013). After 12 hours of pretreatment 32 % of the initial total COD was solubilized into SCOD. Autohydrolysis for 12 hours under anaerobic conditions increased the methane production by 23 % (Carvajal et al., 2013).

1.5 Literature review: anaerobic digestion models

Anaerobic Digestion Model NO.1 (ADM1) developed by the IWA task group for mathematical modelling of anaerobic digestion process is the most comprehensive AD model (Batstone et al., 2002). The theoretical model provides a platform for developing

more process specific models. Well defined model parameters, and nomenclature have allowed for the standardization of the field. ADM1 includes all four biochemical AD steps: hydrolysis, acidogenesis, acetogenesis and methanogenesis. Disintegration of particulate material before hydrolysis is added to the model (Batstone et al., 2002). The disintegration reaction and the particulate component make the model universal and allow it to be adapted and used for various substrates. Acid-base and liquid gas-transfer physico-chemical reactions are used in the model to calculate pH, hydrogen gas and free ammonia. These are used as variables in the model's inhibition functions (Batstone et al., 2002).

First order kinetics are used to describe the extracellular disintegration and hydrolysis reactions. The empirically determined rate constant is a summation of the impact from multiple factors on hydrolysis; including temperature, pH, and biomass concentration (Eastman & Ferguson, 1981). Substrate level Monod-type kinetics are used to describe the rate of the intracellular processes; rates are modified by non-competitive and empirical inhibition functions (Batstone et al., 2002). Cell growth is determined by a Yield coefficient, which links cell growth to the substrate utilization rate. Cell decay forms particulate material which is recycled back into the process. First order rate kinetics describe the cell decay reaction (Batstone et al., 2002).

Souza et al. used ADM1 to examine autohydrolysis impact on AD of WAS (Souza, Carvajal, Donoso-Bravo, Peña, & Fdz-Polanco, 2013). The biochemical methane potential (BMP) of pretreated WAS and raw WAS was examined to calibrate ADM1. A shortcoming of ADM1 is the gap between model variables and experimentally measured sludge characteristics. The study provides a new sludge COD fractionation method to improve the

gap between the experimental results and the model input variables. Sludge was pretreated at 55℃ with a small oxygen concentration and fed to BMP tests and anaerobic digesters (Souza et al., 2013). In the study, the inert fraction of the total COD was determined based on the BMP biodegradability results. Sludge was divided into a SCOD and particulate COD, which was calculated as the difference between total and SCOD. The biodegradable fraction of the SCOD was assigned to monomer variables: sugars, amino acids and long-chain fatty acids. The biodegradable fraction of the particulate COD was divided among carbohydrates, proteins and lipids. Results show that the model simulation results were a good fit for experimental BMP tests with respect to methane production (Souza et al., 2013). However, parameters estimated using BMP tests resulted in poor modeling of the continuous operation processes, which has also been reported by other studies (Batstone, Tait, & Starrenburg, 2009). Bridging the gap between experimental results and model variables is important. A better method would be to directly input experimental results as model variables. Fractioning the COD into model variables adds another level of complexity and uncertainty to modelling and simulation results. A drawback to calibrating ADM1 using BMP tests is the length of the analysis (25 days) (Souza et al., 2013). In wastewater treatment facilities where the influent to the wastewater treatment facility is constantly changing, the sludge content may change at a rate more rapid than the BMP tests. Thus, results from the BMP tests would not be representative of the true sludge characteristics.

1.6 Research objectives

The objectives of this study are to develop a model that can be easily used by operators in wastewater treatment plants and industry to model AD and pretreatment processes. To overcome the limitations of existing models, the number of model variables must be reduced, theoretical model input variables such as proteins, carbohydrates and lipids must be replaced with variables that can be measured using standard sludge characterization analysis. Additionally, the hydrolysis rate equations must be modified to more accurately model non-steady state digesters. In the first part of the study (Chapter 2), a new AD model was developed using the ADM1 framework to more accurately model hydrolysis reactions. The model was generated by reducing the number of model variables, modifying the hydrolysis rate equations (such that they account for fermenting microorganism concentrations), and changing the model input variables to variables from well measured sludge characteristics. In the second part of this study (chapter 3), the objective was to evaluate the performance of an enzymatic hydrolysis pretreatment process and to evaluate the impact of temperature and time on hydrolysis.

1.7 References

ANDREWS, J. F., & GRAEF, S. P. (1971). Dynamic Modeling and Simulation of the Anaerobic Digestion Process (pp. 126–162). https://doi.org/10.1021/ba-1971-0105.ch008

APHA/AWWA/WEF. (2012). Standard Methods for the Examination of Water and Wastewater. *Standard Methods*, 541. https://doi.org/ISBN 9780875532356

Ariunbaatar, J., Panico, A., Esposito, G., Pirozzi, F., & Lens, P. N. L. (2014). Pretreatment methods to enhance anaerobic digestion of organic solid waste. *Applied Energy*, *123*, 143–156. https://doi.org/10.1016/j.apenergy.2014.02.035

Barnard, J. L., Coleman, P., & Weston, P. (2002). THERMAL HYDROLYSIS OF A SLUDGE PRIOR TO ANAEROBIC DIGESTION. *Proceedings of the Water Environment Federation*, *2002*(3), 442–451. https://doi.org/10.2175/193864702785301952

Batstone, D. J., Keller, J., Angelidaki, I., Kalyuzhnyi, S. V., Pavlostathis, S. G., Rozzi, A., … Vavilin, V. A. (2002). The IWA Anaerobic Digestion Model No 1 (ADM1). *Water Science and Technology*, *45*(1), 65–73. https://doi.org/10.2166/wst.2008.678

Batstone, D. J., Tait, S., & Starrenburg, D. (2009). Estimation of hydrolysis parameters in full-scale anerobic digesters. *Biotechnology and Bioengineering*, *102*(5), 1513–1520. https://doi.org/10.1002/bit.22163

Blumensaat, F., & Keller, J. (2005). Modelling of two-stage anaerobic digestion using the IWA Anaerobic Digestion Model No. 1 (ADM1). *Water Research*, *39*(1), 171–183. https://doi.org/10.1016/j.watres.2004.07.024

Boubaker, F., & Ridha, B. C. (2008). Modelling of the mesophilic anaerobic co-digestion of olive mill wastewater with olive mill solid waste using anaerobic digestion model No. 1 (ADM1). *Bioresource Technology*, *99*(14), 6565–6577. https://doi.org/10.1016/j.biortech.2007.11.035

Bougrier, C., Delgenès, J. P., & Carrère, H. (2008). Effects of thermal treatments on five different waste activated sludge samples solubilisation, physical properties and anaerobic digestion. *Chemical Engineering Journal*, *139*(2), 236–244. https://doi.org/10.1016/j.cej.2007.07.099

Carrère, H., Bougrier, C., Castets, D., & Delgenès, J. P. (2008). Impact of initial biodegradability on sludge anaerobic digestion enhancement by thermal pretreatment. *Journal of Environmental Science and Health - Part A Toxic/Hazardous Substances and Environmental Engineering*, *43*(13 SPEC. ISS.), 1551–1555. https://doi.org/10.1080/10934520802293735

Carrère, H., Dumas, C., Battimelli, A., Batstone, D. J., Delgenès, J. P., Steyer, J. P., &

Ferrer, I. (2010). Pretreatment methods to improve sludge anaerobic degradability: A review. *Journal of Hazardous Materials*, *183*(1–3), 1–15. https://doi.org/10.1016/j.jhazmat.2010.06.129

Carvajal, A., Peña, M., & Pérez-Elvira, S. (2013). Autohydrolysis pretreatment of secondary sludge for anaerobic digestion. *Biochemical Engineering Journal*, *75*, 21–31. https://doi.org/10.1016/j.bej.2013.03.002

Chen, Y., Cheng, J. J., & Creamer, K. S. (2008). Inhibition of anaerobic digestion process: A review. *Bioresource Technology*. https://doi.org/10.1016/j.biortech.2007.01.057

Climent, M., Ferrer, I., Baeza, M. del M., Artola, A., Vázquez, F., & Font, X. (2007). Effects of thermal and mechanical pretreatments of secondary sludge on biogas production under thermophilic conditions. *Chemical Engineering Journal*, *133*(1–3), 335–342. https://doi.org/10.1016/j.cej.2007.02.020

Demirel, B., & Yenigün, O. (2002). Two-phase anaerobic digestion processes: A review. *Journal of Chemical Technology and Biotechnology*, *77*(7), 743–755. https://doi.org/10.1002/jctb.630

Eastman, J. a, & Ferguson, J. F. (1981). Solubilization of particulate organic carbon during the acid phase of anaerobic digestion. *Journal of the Water Pollution Control Federation*, *53*(3), 352–366. https://doi.org/10.2307/25041085

Ghosh, S., Conrad, J. R., & Klass, D. L. (1975). Anaerobic acidogenesis of wastewater sludge. *Journal of the Water Pollution Control Federation*, *47*(1), 30–45. Retrieved from http://www.scopus.com/inward/record.url?eid=2-s2.0-0016428893&partnerID=tZOtx3y1

Grady, C. P. L. G., Daigger, G. T., Love, N. G., & Filipe, C. D. M. (2011). *Biological Wastewater Treatment, Third Edition* (3, revised ed.). IWA Publishing. Retrieved from https://books.google.ca/books?id=stjLBQAAQBAJ&dq=biological+methods+of+wastewater+treatment+third+edition&lr=&source=gbs_navlinks_s

Graja, S., Chauzy, J., Fernandes, P., Patria, L., & Cretenot, D. (2005). Reduction of sludge production from WWTP using thermal pretreatment and enhanced anaerobic methanisation. *Water Science and Technology*, *52*(1–2).

Jeong, H.-S., Suh, C.-W., Lim, J.-L., Lee, S.-H., & Shin, H.-S. (2005). Analysis and application of ADM1 for anaerobic methane production. *Bioprocess and Biosystems Engineering*, *27*(2), 81–89. https://doi.org/10.1007/s00449-004-0370-4

Keiding, K., Wybrandt, L., & Nielsen, P. H. (2001). Remember the water - A comment on EPS colligative properties. *Water Science and Technology*, *43*(6), 17–23.

Klein, D. R. (2016). *Organic Chemistry, 3rd Edition.* New York : Wiley. Retrieved from http://www.worldcat.org/title/organic-chemistry-3rd-edition/oclc/973190010

Labatut, R. a, Angenent, L. T., & Scott, N. R. (2014). Conventional mesophilic vs. thermophilic anaerobic digestion: a trade-off between performance and stability? *Water Research*, *53*, 249–58. https://doi.org/10.1016/j.watres.2014.01.035

Langlois, S. (2017). Quebec's Organics Disposal Ban Strategy Webinar – NZWC Food Working Group. Retrieved from http://www.nzwc.ca/webinars/Documents/SophieLanglois-Blouin_Webinar_Dec-7-2017-v3f.pdf

Madigan, M. T. (2014). *Brock biology of microorganisms* (14th edition /). Retrieved from http://www.worldcat.org/title/brock-biology-of-microorganisms/oclc/861647261

Nazari, L., Yuan, Z., Santoro, D., Sarathy, S., Ho, D., Batstone, D., … Ray, M. B. (2017). Low-temperature thermal pre-treatment of municipal wastewater sludge : Process optimization and effects on solubilization and anaerobic degradation. *Water Research*, *113*, 111–123. https://doi.org/10.1016/j.watres.2016.11.055

Neyens, E., Baeyens, J., Dewil, R., & De Heyder, B. (2004). Advanced sludge treatment affects extracellular polymeric substances to improve activated sludge dewatering. *Journal of Hazardous Materials*, *106*(2–3), 83–92. https://doi.org/10.1016/j.jhazmat.2003.11.014

Noike, T., Endo, G., Chang, J. -E, Yaguchi, J. -I, & Matsumoto, J. -I. (1985). Characteristics of carbohydrate degradation and the rate-limiting step in anaerobic digestion. *Biotechnology and Bioengineering*, *27*(10), 1482–1489. https://doi.org/10.1002/bit.260271013

Nosrati, M., Amani, T., & Sreekrishnan, T. R. (2011). Thermophilic Anaerobic Digestion of Waste Activated Sludge versus Mesophilic Anaerobic Digestion.

Pesante, P. N. S., & Vidal, M. V. G. (2016). Developments in pre-treatment methods to improve anaerobic digestion of sewage sludge. *Reviews in Environmental Science and Bio/Technology*, *15*(2), 173–211. https://doi.org/10.1007/s11157-016-9396-8

Raszka, A., Chorvatova, M., & Wanner, J. (2006). The role and significance of extracellular polymers in activated sludge. Part I: Literature review. *Acta Hydrochimica et Hydrobiologica*, *34*(5), 411–424. https://doi.org/10.1002/aheh.200500640

Rea, J. (2014). Kinetic Modeling and Experimentation of Anaerobic Digestion. *Bachelor's Thesis*, 1–58.

Rosen, C., & Jeppsson, U. (2006). Aspects on ADM1 Implementation within the BSM2 Framework. *Technical Report*, 1–37.

Souza, T. S. O., Carvajal, A., Donoso-Bravo, A., Peña, M., & Fdz-Polanco, F. (2013). ADM1 calibration using BMP tests for modeling the effect ofautohydrolysis pretreatment on the performance ofcontinuous sludge digesters. *Water Research*, *47*(9), 3244–3254. https://doi.org/10.1016/j.watres.2013.03.041

Tenney, M. W., & Stumm, W. (1965). Chemical flocculation of microorganisms in biological waste treatment. *Journal - Water Pollution Control Federation*, *37*(10), 1370–1388. https://doi.org/10.2307/25035388

Toreci, I., Kennedy, K. J., & Droste, R. L. (2009). Evaluation of continuous mesophilic anaerobic sludge digestion after high temperature microwave pretreatment. *Water Research*, *43*(5), 1273–1284. https://doi.org/10.1016/j.watres.2008.12.022

Vavilin, V. A., Rytov, S. V., & Lokshina, L. Y. (1996). A description of hydrolysis kinetics in anaerobic degradation of particulate organic matter. *Bioresource Technology*, *56*(2–3), 229–237. https://doi.org/10.1016/0960-8524(96)00034-X

Vlyssides, A. G., & Karlis, P. K. (2004). Thermal-alkaline solubilization of waste activated sludge as a pre-treatment stage for anaerobic digestion. *Bioresource Technology*, *91*(2), 201–206. https://doi.org/10.1016/S0960-8524(03)00176-7

Walker, J., Knight, L., & Stein, L. (1994). A Plain English Guide to the EPA Part 503 Biosolids Rule, (September), 183. Retrieved from water.epa.gov/scitech/wastetech/biosolids/503pe_index.cfm

Wanner, J. (1994). *Activated sludge bulking and foaming control*. Technomic Pub. Retrieved from https://www.crcpress.com/Activated-Sludge-Bulking-and-Foaming-Control/Wanner/p/book/9781566761215

Weemaes, M., Grootaerd, H., Simoens, F., & Verstraete, W. (2000). Anaerobic digestion of ozonized biosolids. *Water Research*, *34*(8), 2330–2336. https://doi.org/10.1016/S0043-1354(99)00373-5

Werker, A. G., Carlsson, M., Morgan-Sagastume, F., Le, M. S., & Harrison, D. (2007). Full Scale Demonstration and Assessment of Enzymic Hydrolysis Pre-Treatment for Mesophilic Anaerobic Digestion of Municipal Wastewater Treatment Sludge. *Proceedings of the Water Environment Federation*, *2007*(13), 5406–5423. https://doi.org/10.2175/193864707787969504

Yan, S., Miyanaga, K., Xing, X. H., & Tanji, Y. (2008). Succession of bacterial community and enzymatic activities of activated sludge by heat-treatment for reduction of excess sludge. *Biochemical Engineering Journal*, *39*(3), 598–603. https://doi.org/10.1016/j.bej.2007.12.002

2 Modelling the hydrolysis of waste activated sludge under thermophilic pretreatment conditions

2.1 Introduction

Anaerobic digesters are used for sludge stabilization, solids reduction and pathogen inactivation, to reduce the cost of sludge disposal, by increasing the number of disposal options and reducing the volume of sludge (Grady et al., 2011). Anaerobic digestion (AD) is a multi-step biological process where particulate organics are broken-down and converted to biogas (Ariunbaatar et al., 2014). Hydrolysis of particulate organics into soluble organics is the rate limiting step in the process; thus, increasing the rate of hydrolysis has the potential to increases the overall rate of AD (Noike et al., 1985). Hydrolysis can be isolated and accelerated using pretreatment processes.

Temperature impacts the kinetics of the biochemical conversion pathways that control the digestion process. The standard operating temperature of most anaerobic digesters is around 37℃. It is the optimal operating temperature for methanogens, and the temperature that ensures process stability (Labatut et al., 2014) (Chen et al., 2008). At higher temperatures, hydrolysis reactions are more rapid in the digester, but operating stability is lost. Rapid hydrolysis reactions lead to a build up of intermediate substrates such as volatile fatty acids, and ammonia which can result in the inhibition of methanogenesis reactions, and digester instability (Chen et al., 2008). Two-phase anaerobic digestion processes optimize the operating conditions, for rapid hydrolysis in the first-phase and stable methanogenesis in the second-phase (Demirel & Yenigün, 2002). Sludge

pretreatment processes increase the extent and rate of digestion. Thermal pretreatment techniques are favoured for their ability to rapidly hydrolyze volatile suspended solids (VSS) into soluble substrate; resulting in shorter overall digestion time, larger digester capacity, increased biogas generation and improved pathogen inactivation (Barnard, Coleman, & Weston, 2002) (Toreci et al., 2009). Thermal hydrolysis describes pretreatment processes operating at temperatures above 100℃, while processes operating at temperatures below 100℃ are referred to as low-temperature thermal hydrolysis processes (Nazari et al., 2017). The advantages of operating at temperatures below 100℃ include reduced energy costs, and greater microbial activity.

Anaerobic digestion models are used to improve process stability, operation, and design. Over the years simple models such as the one developed Andrews et al. have evolved into comprehensive models like the International Water Association Anaerobic Digestion Model NO.1 (ADM1) (ANDREWS & GRAEF, 1971) (Batstone et al., 2002). ADM1 is a theoretical model that describes both the physico-chemical and biochemical reactions that take place in anaerobic digesters (Batstone et al., 2002). ADM1 can be used to track the breakdown of individual substrates, the reduction in solids, the rate of methane production and to calculate the overall volume of biogas generated. ADM1 is often used as the framework for developing new process specific models. Applications include modelling the AD of olive mill wastewater, and a two-stage anaerobic digestion process for treating municipal sludge (Boubaker & Ridha, 2008) (Blumensaat & Keller, 2005). ADM1 uses a large number of variables and parameters, that are challenging to measure and poorly represented by standard sludge analysis techniques (Jeong, Suh, Lim, Lee, &

Shin, 2005). For these reasons industrial application of ADM1 is limited. To overcome this challenge, Souza et al. used biodegradability data from biochemical methane potential (BMP) tests to propose a simplified chemical oxygen demand (COD) fractioning method to define model variables (Souza et al., 2013). However, BMP tests are time consuming and would not be suitable for applications where the sludge characteristics are constantly changing, such as municipal sludge.

Temperature, pH, and fermenting bacteria concentrations are all factors that impact hydrolysis reactions (Eastman & Ferguson, 1981). AD models including ADM1, sum up the impact of all the factors and represent them using an empirically determined first-order kinetic constant k_{hyd} (Batstone et al., 2002). ADM1 assumes that k_{hyd} is independent of digester temperature, and that the hydrolysis reaction is independent of microorganism concentration (Batstone et al., 2002). Both assumptions can be justified for a digester operated at steady-state, a stable pH, and a constant fermenter bacteria concentration. However, the concentration of hydrolytic enzyme secreting fermenting bacteria constantly changes in a batch digester and this change must be factored into the hydrolysis rate equation. k_{hyd} must also be modified according to operating temperature, this is most important when modeling hydrolysis in a high temperature AD pretreatment process.

Improved understanding of hydrolysis will allow for the design, assessment and building of pretreatment processes that will successfully increase the rate of hydrolysis reactions.

The objectives of this study are to:

I. Determine if the volatile suspended solids can be divided into multiple fractions based on volatility,
II. Assess the impact of thermophilic (55℃) pretreatment on hydrolysis,
III. Replace the hydrolysis reaction of ADM1 with the hydrolysis of the volatile suspended solids fractions,
IV. Reduce the number of processes and variables in ADM1,
V. Compare the model to experimental results, and determine kinetic parameters

2.2 Methods and analysis

2.2.1 Experimental methods

The experiments were carried out in a lab-scale anaerobic digester, built using a 250-mL glass bottle. The digester was operated at a thermophilic temperature of 55℃, using incubators for temperature control. The reactor was operated for a total of four days and was sampled at 2 hours, 5 hours, 1 day, 2 days, and 4 days. Biogas was collected using a gas collection bag (2 L capacity, Cali-5 Bond, Calibrated Instruments Inc, NY), to measure gas volume and composition.

The reactor was fed thickened waste activated sludge (TWAS) from a local wastewater treatment facility in Hamilton, Ontario. In the lab TWAS was stored for a period of less then four days at 4℃ prior to use. The characteristics of the sludge collected varied between the two experiments (Table 2.1). With a working volume of 200 mL, the digester was fed 190 mL of thickened WAS and 10 mL of inoculum from a lab-scale

inoculum reactor, operated for 8 months at a temperature of 55℃ and a sludge retention time (SRT) of 20 days. The inoculum reactor operated under continuous batch mode, was fed with the same thickened sludge as the one used for the test digester. The TWAS was warmed up to a temperature of 55℃ over two hours prior to starting the experiment. This was done to avoid a thermal shock to the inoculum used. The digester was purged with inert nitrogen gas and the gas bags were initially filled with 60 mL of nitrogen gas, to avoid a vacuum within the digester when sampling.

Table 2.1: Characteristics of TWAS, warmed to a temperature of 55℃ over two hours prior to pretreatment.

Sludge	I	II
TCOD (g/L)	42.5	48.3
SCOD (g/L)	4.3	5.7
TSS (g/L)	38.1	37.5
VSS (g/L)	27.7	29.0
VSS-505 (g/L)	4.4	5.2
VSS-350 (g/L)	17.9	18.7
VSS-205 (g/L)	5.4	5.1
pH	7.30	6.85

2.2.2 Analytical methods

Analysis included measuring the total solids (TS), volatile solids (VS), total COD (TCOD) and soluble COD (SCOD) according to the standard methods (APHA/AWWA/WEF, 2012). The SCOD was measured after filtering a 2 mL sample using a 1.5 µm filter paper (934-AH Glass Microfiber Filters, GE Healthcare Biosciences) and diluting the sample by a factor of 12. Sludge pH (SevenMulti, Mettler Toledo) was also measured throughout the four days and was found to be neutral (6.8 to 7.9). Biogas collected was analysed for CH_4, CO_2, and N_2 using a thermal conductivity detector-gas

chromatograph (TCD-GC) (SRI 8610C, SRI Instruments, USA). The TCD-GC used a RESTEK packed column (Restek Corporation, PA) and helium as the carrier gas to separate out the gases. The biogas volume was measured using a water displacement method.

Model variables were measured throughout the experiment by modifying the standard suspended solids analysis method. Volatile suspended solids were divided into three fractions: X_{505}, X_{350}, and X_{205}, representing the solids that volatilize at temperatures of 505℃, 350℃, and 205℃ respectively. The volatile fractions were measured by filtering a diluted 2 mL sample of TWAS using a 1.5 μm filter. The filters were then dried over night and sequentially volatilized at each of the three temperatures to determine the various volatile fractions. The analysis was carried out in duplicates for each sample analysed.

2.3 Numerical model development and implementation of hydrolysis digestion model (HDM)

The model structure describes the sequential hydrolysis of volatile suspend solids, the acidogenesis of soluble organics, and the methanogenesis steps of anaerobic digestion (Figure 2.1). Biodegradability of organics can be related to volatility, which increases throughout the AD processes. Hydrolysis of particulate proteins, lipids, and long chain fatty acids described in ADM1 are replaced by the extracellular hydrolysis of the volatile suspended solids fractions X_{505}, X_{350} and X_{205}. Mass sequentially flows from the low volatile suspended solids fraction (X_{505}), to the moderately volatile solids fraction (X_{350}), and further to the high volatile (X_{205}). The product of the hydrolysis reactions is S_{org}, represented in ADM1 by several variables including amino acids, sugars and short chain fatty acids. In the acidogenesis step, fermenters (X_F) rapidly convert the S_{org} to volatile

fatty acids (S_{VFA}) and hydrogen gas (S_{h_2}). Methanotrophic microorganisms X_{VFA} and X_{h_2} convert S_{VFA} and S_{h_2} to biomethane (S_{CH_4}) in the methanogenesis step. The rate equations for the methanogenesis reactions used in HDM are identical to those used in ADM1. Monod-type kinetics are used to describe the substrate utilization of soluble fractions S_{org}, S_{VFA}, and S_{h_2}.

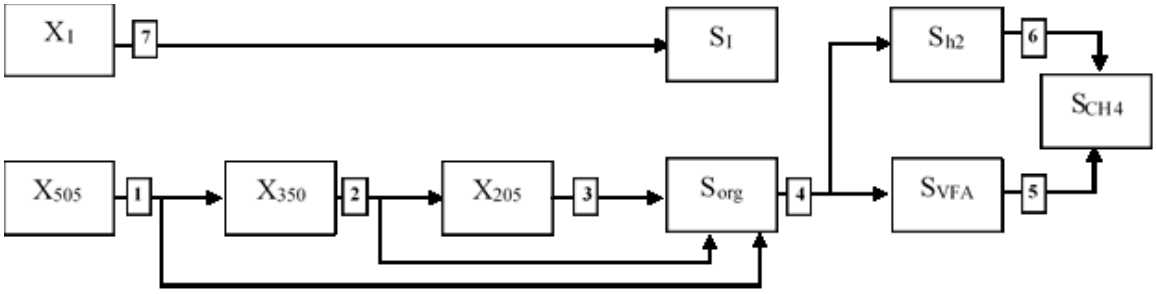

Figure 2.1: Biochemical processes of hydrolysis digestion model (HDM); (1-3) sequential hydrolysis of the volatile suspended solids; (4) acidogenesis of soluble organics; (5) acetoclastic methanogenesis; (6) hydrogenotrophic methanogenesis; (7) hydrolysis of inert particulate organics.

Vavilin et al. suggests that microorganisms attach to solid particles, excrete enzymes that breakdown the particle, and use the soluble substrates broken down by the enzyme for cell growth (Vavilin et al., 1996). In this mechanism, hydrolysis is dependent on the concentration of enzymes in the digester, which is directly proportional to the concentration of fermenting bacteria in the digester. Since the digester is operated in batch mode, the concentration of fermenters will be a limiting factor initially and this limitation must be accounted for by the hydrolysis rate equations, Equation 1, Equation 2 and Equation 3. Mathematically Vanillin et al. describes the two-phase model using a fermenter

saturation concentration X_F^* (Vavilin et al., 1996). At a fermenter concentration below the saturation concentration X_F^*, hydrolysis is limited by a value X_F. At a concentration equal to or greater than X_F^*, it is assumed that the digester is saturated with fermenting bacteria and hydrolysis occurs at a fermenter concentration X_F^*.

$$\frac{dX_{505}}{dt}\Big|_{hydrolysis} = k_{hyd,505}X_{505}X_F \quad (1)$$

$$\frac{dX_{350}}{dt}\Big|_{hydrolysis} = k_{hyd,350}X_{350}X_F \quad (2)$$

$$\frac{dX_{205}}{dt}\Big|_{hydrolysis} = k_{hyd,205}X_{205}X_F \quad (3)$$

A non-steady state model was developed to simulate the rate of solids destruction, and microbial growth expected in the batch digester. The model's three major steps of hydrolysis, acidogenesis, and methanogenesis are described using 10 processes, 12 variables, and 32 stoichiometric and kinetic parameters (Table 2.2). ASM1 matrix format is used to represent the biochemical reactions of HDM (Table A1). The finite difference method was used to convert the system of differential equations into algebraic equations, that were solved implicitly using fixed-point iteration numerical method. A convergence criterion of (10^{-16}) was used solve the system of nonlinear equations. The non-steady state model was implemented and solved using visual basic application (VBA).

Table 2.2: Kinetic parameters, rates and stoichiometric coefficients used in mathematical simulation of HDM.

Model parameter	Symbol	Value	Range	Unit
Max. specific hydrolysis rate of the low volatile suspended solids fraction	$k_{hyd,505}$	0.65	0.25 – 0.15	$L\ gCOD_X^{-1}d^{-1}$
Max. specific hydrolysis rate of the moderately volatile suspended solids fraction	$k_{hyd,350}$	0.31	0.2 – 1.2	$L\ gCOD_X^{-1}d^{-1}$
Max. specific hydrolysis rate of the high volatile suspended solids fraction	$k_{hyd,205}$	0.75	0.29 – 0.9	$L\ gCOD_X^{-1}d^{-1}$
Max. specific soluble organics utilization rate	k_{org}	5	5 – 20	d^{-1}
Max. specific volatile fatty acids methanogenesis rate	k_{VFA}	13	11 – 25	d^{-1}
Max. specific hydrogenotrophic methanogenesis rate	k_{h_2}	35	35	d^{-1}
Fermenter decay rate	k_{dec,X_F}	0.013	0.013 – 0.04	d^{-1}
Volatile fatty acid degraders decay rate	$k_{dec,X_{VFA}}$	0.05	0.02 – 0.06	d^{-1}
Hydrogenotrophic methanogens decay rate	$k_{dec,X_{H_2}}$	0.02	0.02 – 0.04	d^{-1}
Max. specific hydrolysis rate of inert suspended solids	k_{hyd,X_I}	0.003	0.003 – 0.01	$L\ gCOD_X^{-1}d^{-1}$
Half-saturation value for soluble organics utilization	$K_{S,Org}$	0.7	0.3 – 0.9	$gCOD_S\ L^{-1}$
Half-saturation value for volatile fatty acids methanogenesis	$K_{S,VFA}$	0.3	0.25 – 0.45	$gCOD_S\ L^{-1}$
Half-saturation value for hydrogenotrophic methanogenesis	K_{S,H_2}	5×10^{-5}	-	$gCOD_S\ L^{-1}$
Fermenter saturation concentration	F^*	9	6 – 15	$gCOD_X\ L^{-1}$
Yield of fermenters	$Y_{S_{Org}}$	0.4	0.08 – 0.4	$gCOD_X\ gCOD_S^{-1}$
Yield of volatile fatty acid degraders	$Y_{S_{VFA}}$	0.05	0.04 – 0.06	$gCOD_X\ gCOD_S^{-1}$
Yield of hydrogenotrophic methanogens	$Y_{S_{H_2}}$	0.06	0.06	$gCOD_X\ gCOD_S^{-1}$
Fraction of moderately volatile suspended solids from low volatile suspended solids	$f_{505,350}$	0.91	0.5 – 0.99	-
Fraction of soluble organics from low volatile suspended solids	$f_{505,S_{org}}$	0.09	0.01 – 0.5	-
Fraction of highly volatile solids from moderately volatile suspended solids	$f_{350,205}$	0.81	0.4 – 0.99	-
Fraction soluble organics from moderately volatile suspended solids	$f_{350,S_{Org}}$	0.19	0.01 – 0.6	-
Fraction of soluble organics from highly volatile suspended solids	$f_{205,S_{Org}}$	1	-	-
Fraction of soluble inert from inert suspended solids	f_{X_I,S_I}	0.07	0.03 – 0.1	-
Fraction of inert suspended solids from the decay of fermenters	f_{X_F,X_I}	0.02	0.01 – 0.1	-
Fraction of low volatile suspended solids from the decay of fermenters	$f_{X_F,X_{505}}$	0.98	0.9 – 0.99	-
Fraction of inert suspended solids from the decay of volatile fatty acid degraders	f_{X_{VFA},X_I}	0.02	0.01 – 0.1	-
Fraction of low volatile suspended from the decay of volatile fatty acid degraders	$f_{X_{VFA},X_{505}}$	0.98	0.9 – 0.99	-
Fraction of inert suspended solids from the decay of hydrogenotrophic methanogens	$f_{X_{H_2},X_I}$	0.02	0.01 – 0.1	-
Fraction of low volatile suspended solids from the decay of hydrogenotrophic methanogens	$f_{X_{H_2},X_{505}}$	0.98	0.9 – 0.99	-
Fraction of microorganisms that is low volatile suspended solids	$f_{X_M,X_{505}}$	0.13	0.1 – 0.25	-
Fraction of microorganisms that is moderately volatile suspended solids	$f_{X_M,X_{350}}$	0.62	0.4 – 0.7	-
Fraction of microorganisms that is highly volatile suspended solids	$f_{X_M,X_{205}}$	0.25	0.1 – 0.3	-

2.4 Sensitivity analysis

Sensitivity analysis was used to determine the rate limiting hydrolysis reaction. The focus variables in the analysis were VSS (sum of X_{505},X_{350}, and X_{205}.), SCOD (sum of S_{org}, S_I, and S_{VFA}), and methane gas. VSS and SCOD were used because they are experimental indicators of hydrolysis. Methane gas was used to examine parameter impact on the overall digestion process. Hydrolysis rate constants $k_{hyd,505}$, $k_{hyd,350}$, and $k_{hyd,205}$ were the parameters examined. Sensitivity value (SV) was calculated according to Equation 4.

$$SV = \frac{S_{SENS}}{S_{STD}} \tag{4}$$

S_{SENS} is the simulation value of the focus variable using the new hydrolysis parameter, and S_{STD} is the simulation value of the focus variable at the standard hydrolysis parameter values used in Table 2.2. SV was examined at parameter values of 10, 50, 200, and 1000% of the standard parameter value.

2.5 Results and discussion

2.5.1 Model validation

HDM accurately simulates the rapid increase in experimental SCOD during the first day of pretreatment, the peak at two days, and the gradual decrease from day two to day four (Figure 2.2a). The increase in SCOD is an indicator that particulate organics were hydrolyzed in the pretreatment digester. Experimental results show that the rate of hydrolysis was highest during the first two hours of pretreatment. Comparing SCOD measured in sludge one (SI) and two (SII), it is clear the SCOD values in SII are consistently greater than those in SI; thus, the sludge in SII was more biodegradable than the sludge in SII. In this study, the time sludge was sampled from the wastewater treatment plant (WWTP) was the only variable between SI and SII; thus, sludge characteristics in WWTPs are constantly changing.

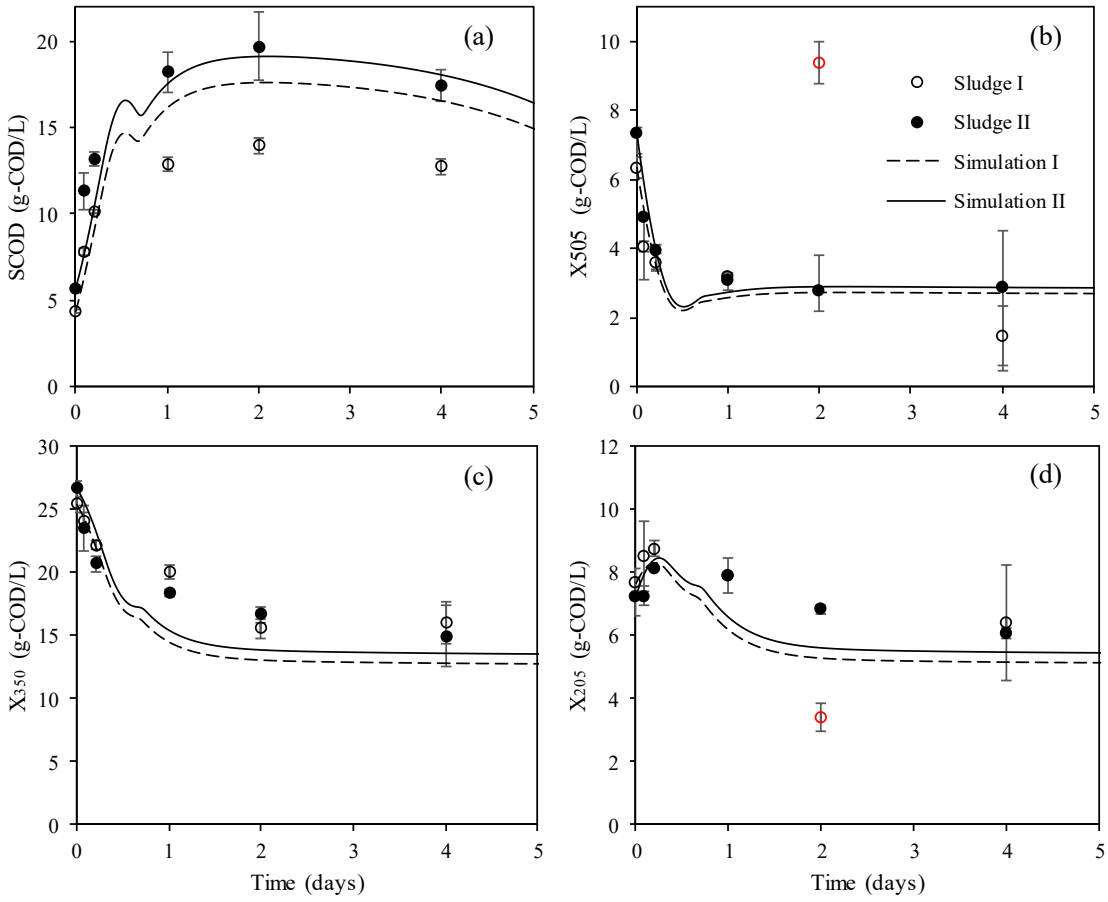

Figure 2.2: Comparing the experimental and mathematical simulation results of experiments on sludge one and two: (a) soluble COD concentration; (b) low volatile suspended solids; (c) moderately volatile suspended solids; (d) highly volatile suspended solids. The experiments were run for four days, while the simulations show results for a five-day period. The kinetic constants used are listed in Table 2.2 and the influent sludge compositions for both simulations are listed in Table 2.3. The two simulations vary only by initial sludge composition. The error bars represent standard deviation (n = 2). The experimental points represent outliers from the overall trend.

Model SCOD is a summation of the soluble model variables: S_I, S_{org}, and S_{VFA}. S_{org} initially increases to a maximum value after nine hours of rapid VSS hydrolysis (Figure 2.3a). The peak in the S_{org} causes a small peak in the SCOD simulation curve (Figure 2.2a). At a fermenting bacteria concentration X_F^*, hydrolysis is no longer limited by

enzyme concentration, but rather by enzyme kinetics. Although the rate of hydrolysis becomes limited by enzymatic kinetics, the rate of fermentation continues to increase as $X_F > X_F^*$. Rapid fermentation reactions convert S_{org} into $S_{VFA}$and S_{h_2} at a rate more rapid then it is generated. S_{org} decreases to less than 1 mg-COD/L after 9 hours (Figure 2.3a).

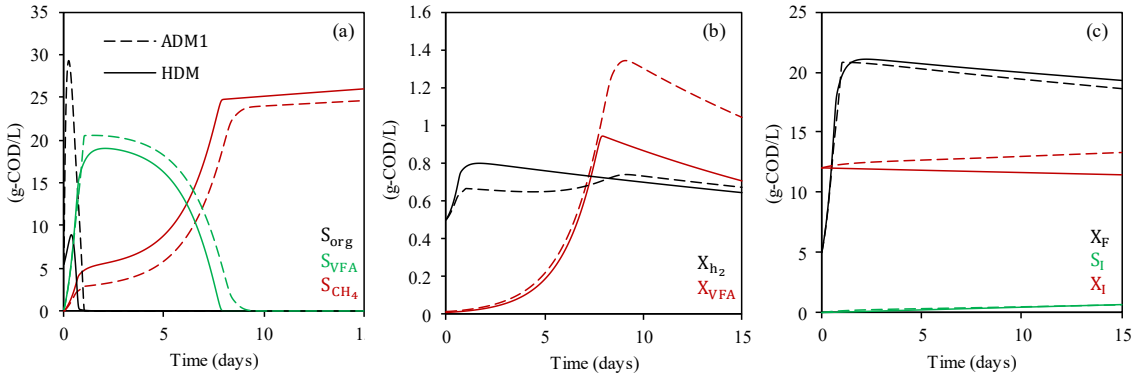

Figure 2.3: Comparison of simulation results between HDM (solid line), and ADM1 (dashed line): (a) methane gas, volatile fatty acids, and soluble organic monomers; (b) volatile fatty acid degraders, and hydrogenotrophic methanogens; (c) fermenters, inert suspended solids, and soluble inerts. Simulations were run for 15 days. The kinetic constants used are listed in Table 2.2 and Table 2.4. The initial sludge composition values used are listed in Table 2.3 (Sludge II), and Table 2.5.

S_{VFA} is initially built up in the system, maximized at two days, and gradually decreases to zero (Figure 2.3a). The plot for S_{VFA} has a similar shape to that of SCOD, and levels off to a value of less than 1 g-COD/L after eight days. At 8 days X_{VFA} peaks, converting the S_{VFA} to methane gas at a rapid rate forcing its concentration to stay lower than 1 g-COD/L. The volatile fatty-acid concentration was not experimentally measured; However, given the rapid rate of fermentation reactions (<1 day), and the inoculum sludge

introduced initially to the reactor, the SCOD measured value after a retention time of 9 hours can be attributed mostly to S_{VFA} (Grady et al., 2011).

The extent and rate of X_{505} degradation was not expected given the fraction's low volatility (Figure 2.2b). Pretreatment at 55℃ over a period of 4 days resulted in a 73% and 74% reduction of X_{505} in SII and SI respectively. Much of the X_{505} degradation occurred within the first 2 hours and leveled off to the equilibrium value after only 5 hours. A regression analysis on both SII and SI shows that zero is between the upper and lower 95 % confidence interval for the slope of the line between five hours and four days. This means that X_{505} did not change after five hours of pretreatment. HDM simulations are consistent with the experimental plots for X_{505}, showing the initial rapid drop and the leveling off after five hours.

Active microorganisms X_F, X_{VFA}, and X_{h2} in the sludge cannot be directly measured and are instead indirectly measured by VSS analysis. The model has separate variables for the active microorganisms, and for the VSS fractions. To compare the model simulations to the experiential results, the VSS fractions from the model must include the microorganism concentrations. The X_{505}, X_{350} and X_{205} simulation values in Figure 2.2 are a combination of the VSS variables and a fraction (f_M) of the microorganisms. f_M was determined by calculating the fraction of the total VSS that each VSS fractions made up at the end of the four days of pretreatment. X_{505} accounted for 12% of the total VSS, X_{350} made up 63%, and X_{205} made up the remaining 25%. This is how the microorganism fractions $f_{M,505}$, $f_{M,350}$, and $f_{M,205}$ were determined (Table 2.2).

Table 2.3: Initial composition of TWAS, used as initial variable values in mathematical simulations of HDM.

Model variable	Symbol	Simulation I (gCOD L^{-1})	Simulation II (gCOD L^{-1})
Soluble organics	S_{Org}	4.2	5.5
Volatile fatty acids	S_{VFA}	1.5×10^{-1}	2×10^{-1}
Hydrogen gas	S_{H_2}	3×10^{-6}	3×10^{-6}
Soluble inerts	S_I	1.1×10^{-2}	1.5×10^{-2}
Methane gas	S_{CH_4}	0	0
Low volatile suspended solids	X_{505}	5.6	10
Moderately volatile suspended solids	X_{350}	21.9	19.8
High volatile suspended solids	X_{205}	6.3	5.9
Inert suspended solids	X_I	14.8	12
Fermenters	X_F	5	5
Volatile fatty acid degraders	X_{VFA}	1×10^{-2}	1×10^{-2}
Hydrogenotrophic methanogens	X_{H_2}	5×10^{-1}	5×10^{-1}

*Sludge composition values were selected to match measured values, with VSS fractions converted to COD using the conversion factor of 1.42 g-COD/g-VSS. Microorganism concentrations were selected based on the concentrations fractions suggested for typical waste activated sludge.

X_{350} was the largest VSS fraction, and it gradually decreased over the four days of pretreatment. Although gradual, the hydrolysis of X_{350} greatly impacted the entire process. Both simulations capture the overall shape of the hydrolysis curves from SII and SI but are slightly shifted down (Figure 2.2c). This means that X_{350} was hydrolyzed at a more rapid rate in the model. The overall reduction in X_{350} over the four days is 37% in SII and 36% in SII; overestimated by simulations I and II at a reduction of 42% and 50% respectively. Regression analysis on the experimental results gives a negative slope. A slope value of zero was not in the range between the upper and lower 95 % confidence intervals, that means the reduction of X_{350} was statistically significant. Additionally, the residual plots for the regression analysis are parabolic; thus, using a linear model to represent the data would not be appropriate. This result confirms the need for factoring in the fermenting microorganism concentration in the hydrolysis rate equations.

X_{205} increased initially and peaked at an SRT of five hours in both experiments. Over the four days of pretreatment, gradual reduction of X_{205} was measured (Figure 2.2d). HDM simulations were consistent with the experimental results and show a gradual decrease of X_{205} over the four days. X_{205} is the most volatile suspended solids fraction, the high volatility was accounted for in the model by assigning it a high hydrolysis rate constant $k_{hyd,205}$. X_{350} is initially much greater than X_{205}; thus, its hydrolysis leads to a build up of X_{205} (Figure 2.2d). The consistent reduction of X_{350} over the four days leads to a gradual decrease in X_{205}, and an overall reduction of only 16% in both SI and SII. The model simulations capture both the initial peak and the overall shape of the curve. However, the simulations predict a slightly more rapid reduction in X_{205}.

The experimental results prove that the VSS can be divided into multiple fractions based on volatility. The fractions are not equal in weight, degrade at different rates and towards different extents. The initial hypothesis was that the extent and rate of degradation would increase with increasing volatility. However, the experimental results suggest otherwise. Simulation results are very close to the experimental results (Figure 2.2); thus, the model can be used to explain the experimental results. Given the sequential flow of mass in the model (Figure 2.1), it is easy to understand why the experimental results obtained are opposite to those predicted. X_{205} can be degrading at a rapid rate, and towards a greater extent however as the product of X_{350} hydrolysis, X_{205} is generated at a rate close to its utilization. Thus, the experimental and simulation results show a lower rate and extent of degradation for X_{205} compared to X_{505}. The slow rate and extent of degradation are not

the result of X_{205} biodegradability properties, but rather how mass flows through the system. Thus, the initial hypothesis can still be true.

2.5.2 Model comparison with ADM1

The volatile suspended solid fractions X_{505}, X_{350}, and X_{205} can not be directly compared with any ADM1 variables. However, model variables S_{org}, S_{VFA}, X_{VFA}, and X_F can be compared to ADM1 variables. The initial variable values used in ADM1 were assigned according to the initial composition of WAS measured. The total VSS measured was converted to COD using a 1.42 g-COD/g-VSS conversion factor; fractioned into fermenters X_{su}, X_{aa} and X_{li}, and particulate solids X_C, X_{ch}, X_{li} and X_{pr} (Table 2.5). Rosen & Jeppsson modeled the digestion of WAS using ADM1, and assigned the greatest influent value to X_{pr} (Rosen & Jeppsson, 2006). X_{pr} is assumed to be high in WAS because it is rich in extracellular polymeric substances, which are composed mainly of proteins and polysaccharides (Tenney & Stumm, 1965).

Table 2.4: Kinetic parameters, rates and stoichiometric coefficients used in ADM1 model mathematical simulations.

Model parameter	Symbol	Value	Unit
First order decay rate of sugar degraders *	$k_{dec,su}$	1.3×10^{-2}	d^{-1}
First order decay rate of amino acid degraders *	$k_{dec,aa}$	1.3×10^{-2}	d^{-1}
First order decay rate of long-chain fatty beta-oxidizers *	$k_{dec,fa}$	1.3×10^{-2}	d^{-1}
First order decay rate of valerate and butyrate beta-oxidizers *	$k_{dec,C4}$	5×10^{-2}	d^{-1}
First order decay rate of propionate beta-oxidizers *	$k_{dec,pro}$	5×10^{-2}	d^{-1}
First order decay rate of acetoclastic methanogens *	$k_{dec,ac}$	5×10^{-2}	d^{-1}
First order decay rate of hydrogenotrophic methanogens *	k_{dec,h_2}	2×10^{-2}	d^{-1}
First order composite disintegration rate	k_{dis}	1	d^{-1}
First order hydrolysis rate	k_{hyd}	10	d^{-1}
Monod Max. specific sugar utilization rate *	k_{su}	5	d^{-1}
Monod Max. specific amino acids utilization rate *	k_{aa}	5	d^{-1}
Monod Max. specific long-chain fatty acids utilization rate *	k_{fa}	5	d^{-1}
Monod Max. specific valerate and butyrate utilization rate *	k_{C4}	13	d^{-1}
Monod Max. specific propionate utilization rate *	k_{pro}	13	d^{-1}
Monod Max. specific acetoclastic methanogenesis rate *	k_{ac}	13	d^{-1}
Monod Max. specific hydrogenotrophic methanogenesis rate	k_{h_2}	35	d^{-1}
Half-saturation value for sugar utilization	$K_{s,su}$	1	$gCOD_S\ L^{-1}$
Half-saturation value for amino acid utilization	$K_{s,aa}$	a 3×10^{-1} [a]	$gCOD_S\ L^{-1}$
Half-saturation value for long-chain fatty acids utilization	$K_{s,fa}$	4×10^{-2}	$gCOD_S\ L^{-1}$
Half-saturation value for valerate and butyrate utilization	$K_{s,C4}$	4×10^{-3}	$gCOD_S\ L^{-1}$
Half-saturation value for propionate utilization	$K_{s,pro}$	3×10^{-1}	$gCOD_S\ L^{-1}$
Half-saturation value for acetoclastic methanogenesis	$K_{s,ac}$	3×10^{-1}	$gCOD_S\ L^{-1}$
Half-saturation value for hydrogenotrophic methanogenesis	K_{s,h_2}	5×10^{-5}	$gCOD_S\ L^{-1}$
Yield of fermenters on sugar *	Y_{su}	4×10^{-1}	$gCOD_X\ gCOD_S^{-1}$
Yield of fermenters on amino acids *	Y_{aa}	4×10^{-1}	$gCOD_X\ gCOD_S^{-1}$
Yield of beta-oxidizers on long-chain fatty acids *	Y_{fa}	4×10^{-1}	$gCOD_X\ gCOD_S^{-1}$
Yield of beta-oxidizers on valerate and butyrate *	Y_{C4}	5×10^{-2}	$gCOD_X\ gCOD_S^{-1}$
Yield of beta-oxidizers on propionate	Y_{pro}	5×10^{-2}	$gCOD_X\ gCOD_S^{-1}$
Yield of acetoclastic methanogens on acetic acid	Y_{ac}	5×10^{-2}	$gCOD_X\ gCOD_S^{-1}$
Yield of hydrogenotrophic methanogens on hydrogen	Y_{h_2}	6×10^{-2}	$gCOD_X\ gCOD_S^{-1}$
Fraction of soluble inerts from composites	$f_{sI,xc}$	1×10^{-1}	-
Fraction of particulate inerts from composites	$f_{xI,xc}$	2×10^{-1}	-
Fraction of carbohydrates from composites	$f_{ch,xc}$	2×10^{-1}	-
Fraction of proteins from composites	$f_{pr,xc}$	2×10^{-1}	-
Fraction of lipids from composites	$f_{li,xc}$	3×10^{-1}	-
Fraction of fatty acids from lipids	$f_{fa,li}$	9.5×10^{-1}	-
Fraction of hydrogen from sugars	$f_{h_2,su}$	1.9×10^{-1}	-
Fraction of butyrate from sugars	$f_{bu,su}$	1.3×10^{-1}	-
Fraction of propionate from sugars	$f_{pro,su}$	2.7×10^{-1}	-
Fraction of acetate from sugars	$f_{ac,su}$	4.1×10^{-1}	-
Fraction of hydrogen from amino acids	$f_{h_2,aa}$	6×10^{-2}	-
Fraction of valerate from amino acids	$f_{va,aa}$	2.3×10^{-1}	-
Fraction of butyrate from amino acids	$f_{bu,aa}$	2.6×10^{-1}	-
Fraction of propionate from amino acids	$f_{pro,aa}$	5×10^{-2}	-
Fraction of acetate from amino acids	$f_{ac,aa}$	4×10^{-1}	-

Parameter values are suggested from Batstone et al. (2002), for a temperature of 55°C.
* Values changed to those suggested in literature and used in the model.

Table 2.5: Initial composition of WAS, used as initial variable values in ADM1 for simulations.

Model parameter	Symbol	Experiment I ($gCOD\ L^{-1}$)
Sugars	S_{su}	9.2×10^{-1}
Amino acids	S_{aa}	3.7×10^{-1}
Long-chain fatty acids	S_{fa}	9.2×10^{-6}
Valerate	S_{va}	5×10^{-2}
Butyrate	S_{bu}	5×10^{-2}
Propionate	S_{pro}	5×10^{-2}
Acetate	S_{ac}	5×10^{-2}
Hydrogen gas	S_{h_2}	1×10^{-8}
Methane gas	S_{CH_4}	0
Soluble inerts	S_I	1.5×10^{-2}
Composites	X_C	2.2
Carbohydrates	X_{ch}	5.6
Proteins	X_{pr}	22.3
Lipids	X_{li}	5.6
Sugar fermenters	X_{su}	1.8
Amino acid fermenters	X_{aa}	1.8
Long-chain fatty acid beta-oxidizers	X_{fa}	1.5
Valerate and butyrate beta-oxidizers	X_{c4}	5×10^{-3}
Propionate beta-oxidizers	X_{pro}	3×10^{-3}
Acetoclastic methanogens	X_{ac}	7×10^{-3}
Hydrogenotrophic methanogens	X_{h_2}	5×10^{-1}
Particulate inerts	X_I	12

*Sludge composition values were selected to match measured values, with VSS fractions converted to COD using the conversion factor of 1.42 g-COD/g-VSS. Other values were taken from Rosen & Jeppsson et al. (2006).

S_{org} peaks at a value of 29.3 g-COD/L and 8.5 g-COD/L in ADM1 and HDM simulation I respectively (Figure 2.3a). The S_{org} value for ADM1 is a summation of S_{su}, S_{aa}, and S_{fa}, all products of the hydrolysis reactions. ADM1 uses a more rapid hydrolysis rate constant compared to HDM and given the high X_{pr} initially, a high concentration of S_{aa} is produced, resulting in a large difference between the S_{org} peak of the two models. In both models S_{org} drops to a value of less than 1 g-COD/L after one day of pretreatment, as fermenters convert S_{org} into S_{VFA} and S_{H2}.

X_F peaks in one day to a concentration where it can use up the soluble monomers at a more rapid rate than they are produced (Figure 2.3c). The X_F in ADM1 is a summation of X_{su}, X_{aa}, and X_{fa}. The kinetic parameters used in the Monod equations describing the monomer utilization process are the same for all fermenters in ADM1 and HDM (Table 2.4) (Table 2.2). The suggested ADM1 Monod maximum specific uptake rate coefficients at 55℃ were in the range of 10 – 70 d^{-1} (Batstone et al., 2002). Simulation results suggest that the uptake rate coefficient is limiting below 5 d^{-1}; moreover, increasing it beyond 5 d^{-1} does not have a significant impact on the rest of the model variables. Thus, it was set to 5 d^{-1} in both models. The yield of fermenters on S_{org} was also modified in both models from the suggested ADM1 range of 0.06 to 0.1 at 55℃ to 0.4 (Batstone et al., 2002). ADM1 suggests little to no sensitivity of other model variables to the yield coefficient under non-steady state conditions (Batstone et al., 2002). However, the simulation results suggest that all model variables are sensitive to this parameter. The suggested yield value results in rapid and complete degradation of all model substrate variables, and their conversion to methane gas in less than five days. This is not consistent with the measured and expected experimental results. Gosh et al. operated a two-phase anaerobic digestion process, and reported a Yield value of 0.4 in the acid-phase (Ghosh, Conrad, & Klass, 1975). Given the pretreatment process used in this study resembles the acid-phase of a two-phase process, the Yield coefficient was set to 0.4. At a higher yield coefficient, fermenters use more of the substrate for cell growth and reproduction, which resulted in a significantly higher and more rapid X_F peak (Figure 2.3c). X_F are considered part of the VSS; a large X_F maintains the VSS fractions high in the simulations, and thus simulations results are more compatible

with experimental results. With a larger X_F, more mass is recycled into the system through cell decay. The cell decay kinetic rate constant for X_F was reduced from the suggested 0.04 d^{-1} value to 0.013 d^{-1} (Batstone et al., 2002). This was also done to maintain a high fermenter concentration. Comparing the simulation results, the two appear to be identical, having the same curve and peak (Figure 2.3c).

The products of fermentation S_{VFA} and S_{h2} are substrates for the methanogenesis step. Hydrogenotrophic methanogens X_{h2} accept electrons from hydrogen gas S_{h_2} to reduce carbon dioxide, and form methane gas. X_{h2} is made up of a diverse groups of *Archaea* species that are robust and grow rapidly (Grady et al., 2011). The process rate equation and kinetic constants used in both models are the ones suggested in ADM1 at 55℃ (Batstone et al., 2002). X_{h_2} rapidly peaks at one day (Figure 2.3b). The value of the peak is not significant in comparison with X_F; however, $S_{h_2}$is the electron carrier in the digestion processes and X_{h_2} is important in driving the reaction forward. Simulation results show that the S_{h_2} peaks to a value of 0.00003 g-COD/L within the first day and then rapidly decreases to a value of near zero. At one day X_{h_2} is sufficient enough to convert S_{h_2} to methane gas. Both models have the same shape for X_{h_2} with ADM1 peaking at a higher value. In ADM1, 29% of WAS becomes hydrogen gas and is converted to methane through hydrogenotrophic methanogenesis (Batstone et al., 2002). In HDM, 22% of all biodegradable solids become hydrogen gas (Table 2.2); thus, explaining the different peaks in the simulations. In the HDM S_{org} is directly converted to methane gas, whereas in ADM1 the methane gas is generated through a series of reactions. Using a smaller fraction, ensures

that the methane generation through hydrogenotrophic methanogenesis is not overestimated by the model early on.

SCFA degraders are responsible for most of the S_{ch4} generation. S_{ch4} increases with increasing X_{VFA} and peaks at eight days. The $X_{VFA}$of ADM1 is a summation of ADM1 variables:X_{c4}, X_{pro}, and X_{ac}. The kinetic parameters used in the rate equations that describe the substrate utilization of these variables were modified to match the ones used in HDM (Table 2.3). The rate of cell death and decay was set to a value of 0.05 d^{-1}, which is higher than the 0.04 value suggested in ADM1 (Batstone et al., 2002). Monod maximum specific uptake rate coefficient was set to 13 d^{-1} also smaller than the suggested ADM1 values (Batstone et al., 2002). The pretreatment process is operated to maximize solubilization; thus, methanogenesis reactions are expected to occur at a slower rate. The modifications in the kinetic parameters are meant to reflect the impact of the operating conditions. X_{VFA} simulations are initially identical, however the plot for HDM peaks earlier at a lower value (Figure 2.3b). The S_{VFA} of ADM1 is the summation of S_{va}, S_{bu}, S_{pro}, and S_{ac} model variables. Simulation results of S_{VFA} are similar for both models. The variable peaks in less than two days and gradually decreases to a value of 0 g-COD/L at around eight days. The time when X_{VFA} reaches a maximum.

The models have a similar methane generation curve with nearly identical curves. HDM uses significantly less variables to describe AD. The variables that are used to describe hydrolysis reactions, are easily measured using the modified standard wastewater characterization analysis.

2.5.3 Sensitivity analysis results

The second hydrolysis reaction was found to govern the pretreatment performance. Focus variables, CH_4, SCOD and VSS were relatively insensitive to changes in the first and third hydrolysis reactions compared to the second hydrolysis reaction. SV for SCOD at 12 hours was 1.10, 1.66, and 1.23 when $k_{hyd,505}$, $k_{hyd,350}$, and $k_{hyd,205}$ were increased by 10 times, respectively (Table 2.6). This result indicates that an increase in $k_{hyd,350}$ can enhance the SCOD production. Similarly, an increase in $k_{hyd,350}$ resulted in a significant decrease in VSS and a substantial increase in CH_4 while an increase in $k_{hyd,505}$ and $k_{hyd,205}$ had a relatively insignificant impact on the focus variables VSS and CH_4. This finding implies that the thermophilic pretreatment should be targeted to enhance the second hydrolysis reaction because the kinetics of hydrolysis reactions are highly dependent on temperature conditions. Operating at temperatures greater than 55℃, can result in higher hydrolysis rate constants. However, there is a limit beyond which the impact of temperature on hydrolysis is not important. This is evident when comparing the sensitivity values of variables when the kinetic parameter is increased by a factor of 2 to those increased by a factor of 10. Thermal hydrolysis processes are energy intensive and minimizing the energy required for pretreatment is important. If a correlation between $k_{hyd,350}$ and temperature is determined, the operating conditions can be optimized with the objectives of increasing the rate of hydrolysis and reducing energy costs. Changes to the SV are most significant within the first 12 hours, showing that after a day the impact is reduced. This means that operating

at higher temperature conditions is most important for the first 12 hours of digestion, and thus not necessary for the entire digestion process.

Table 2.6: Sensitivity of methane gas (CH_4), soluble chemical oxygen demand (SCOD), and the volatile suspended solids (VSS) to kinetic parameters $k_{hyd,505}$, $k_{hyd,350,}$ and $k_{hyd,205}$; at 12 hours, one day, two days, and four days. The kinetic parameters were varied to 10, 50, 200 and 1000% of the original parameter value outlined in (Table 2.2).

	CH_4				SCOD				VSS			
$k_{hyd,505}$	12 hrs	1 d	2 d	4 d	12 hrs	1 d	2 d	4 d	12 hrs	1 d	2 d	4 d
0.065	0.98	0.85	0.90	0.97	0.81	0.85	0.89	0.96	1.11	1.13	1.12	1.05
0.325	0.99	0.97	0.99	1.00	0.93	0.97	0.99	1.00	1.04	1.03	1.01	1.00
0.65	1.00	1.00	1.00	1.00	1.00	1.00	1.00	1.00	1.00	1.00	1.00	1.00
1.3	1.01	1.01	1.00	1.00	1.05	1.02	1.00	1.00	0.97	0.99	1.00	1.00
6.5	1.02	1.02	1.00	1.00	1.10	1.03	1.00	1.00	0.94	0.98	1.00	1.00
$k_{hyd,350}$	12 hrs	1 d	2 d	4 d	12 hrs	1 d	2 d	4 d	12 hrs	1 d	2 d	4 d
0.031	0.74	0.49	0.60	0.80	0.42	0.49	0.57	0.72	1.35	1.46	1.47	1.29
0.155	0.94	0.83	0.94	0.99	0.70	0.84	0.94	0.99	1.17	1.15	1.07	1.01
0.31	1.00	1.00	1.00	1.00	1.00	1.00	1.00	1.00	1.00	1.00	1.00	1.00
0.62	1.03	1.09	1.01	1.00	1.34	1.09	1.01	1.00	0.81	0.92	0.99	1.00
3.1	1.07	1.11	1.01	1.00	1.66	1.11	1.01	1.00	0.63	0.90	0.99	1.00
$k_{hyd,205}$	12 hrs	1 d	2 d	4 d	12 hrs	1 d	2 d	4 d	12 hrs	1 d	2 d	4 d
0.075	0.69	0.58	0.77	0.94	0.41	0.58	0.75	0.92	1.36	1.38	1.27	1.08
0.375	0.95	0.93	0.99	1.00	0.77	0.93	0.99	1.00	1.13	1.07	1.01	1.00
0.75	1.00	1.00	1.00	1.00	1.00	1.00	1.00	1.00	1.00	1.00	1.00	1.00
1.5	1.03	1.03	1.00	1.00	1.14	1.03	1.00	1.00	0.92	0.98	1.00	1.00
7.5	1.05	1.04	1.00	1.00	1.23	1.04	1.00	1.00	0.87	0.97	1.00	1.00

2.6 Conclusions

Sludge was successfully fractioned based on volatility. The various fractions X_{505}, X_{350}, and X_{205} made up different fractions of the total VSS and degraded at different rates. HDM simulations were comparable to the experimentally measure data and ADM1 simulations; thus, the model can be used to predict solubilization after pretreatment at 55℃, given the initial sludge composition. Using less variables, and more accurately defined model inputs. The sensitivity analysis shows that hydrolysis is most sensitive to the second hydrolysis reaction and increasing its rate would increase the overall rate of the AD process. Pretreatment at temperatures above 55℃, to evaluate the temperature impact on $k_{hyd,505}$ and thus the overall process would be beneficial.

2.7 References

ANDREWS, J. F., & GRAEF, S. P. (1971). Dynamic Modeling and Simulation of the Anaerobic Digestion Process (pp. 126–162). https://doi.org/10.1021/ba-1971-0105.ch008

APHA/AWWA/WEF. (2012). Standard Methods for the Examination of Water and Wastewater. *Standard Methods*, 541. https://doi.org/ISBN 9780875532356

Ariunbaatar, J., Panico, A., Esposito, G., Pirozzi, F., & Lens, P. N. L. (2014). Pretreatment methods to enhance anaerobic digestion of organic solid waste. *Applied Energy*, *123*, 143–156. https://doi.org/10.1016/j.apenergy.2014.02.035

Barnard, J. L., Coleman, P., & Weston, P. (2002). THERMAL HYDROLYSIS OF A SLUDGE PRIOR TO ANAEROBIC DIGESTION. *Proceedings of the Water Environment Federation*, *2002*(3), 442–451. https://doi.org/10.2175/193864702785301952

Batstone, D. J., Keller, J., Angelidaki, I., Kalyuzhnyi, S. V., Pavlostathis, S. G., Rozzi, A., … Vavilin, V. A. (2002). The IWA Anaerobic Digestion Model No 1 (ADM1). *Water Science and Technology*, *45*(1), 65–73. https://doi.org/10.2166/wst.2008.678

Blumensaat, F., & Keller, J. (2005). Modelling of two-stage anaerobic digestion using the IWA Anaerobic Digestion Model No. 1 (ADM1). *Water Research*, *39*(1), 171–183. https://doi.org/10.1016/j.watres.2004.07.024

Boubaker, F., & Ridha, B. C. (2008). Modelling of the mesophilic anaerobic co-digestion of olive mill wastewater with olive mill solid waste using anaerobic digestion model No. 1 (ADM1). *Bioresource Technology*, *99*(14), 6565–6577. https://doi.org/10.1016/j.biortech.2007.11.035

Chen, Y., Cheng, J. J., & Creamer, K. S. (2008). Inhibition of anaerobic digestion process: A review. *Bioresource Technology*. https://doi.org/10.1016/j.biortech.2007.01.057

Demirel, B., & Yenigün, O. (2002). Two-phase anaerobic digestion processes: A review. *Journal of Chemical Technology and Biotechnology*, *77*(7), 743–755. https://doi.org/10.1002/jctb.630

Eastman, J. a, & Ferguson, J. F. (1981). Solubilization of particulate organic carbon during the acid phase of anaerobic digestion. *Journal of the Water Pollution Control Federation*, *53*(3), 352–366. https://doi.org/10.2307/25041085

Ghosh, S., Conrad, J. R., & Klass, D. L. (1975). Anaerobic acidogenesis of wastewater sludge. *Journal of the Water Pollution Control Federation*, *47*(1), 30–45. Retrieved from http://www.scopus.com/inward/record.url?eid=2-s2.0-0016428893&partnerID=tZOtx3y1

Grady, C. P. L. G., Daigger, G. T., Love, N. G., & Filipe, C. D. M. (2011). *Biological Wastewater Treatment, Third Edition* (3, revised ed.). IWA Publishing. Retrieved from https://books.google.ca/books?id=stjLBQAAQBAJ&dq=biological+methods+of+wastewater+treatment+third+edition&lr=&source=gbs_navlinks_s

Jeong, H.-S., Suh, C.-W., Lim, J.-L., Lee, S.-H., & Shin, H.-S. (2005). Analysis and application of ADM1 for anaerobic methane production. *Bioprocess and Biosystems Engineering*, *27*(2), 81–89. https://doi.org/10.1007/s00449-004-0370-4

Labatut, R. a, Angenent, L. T., & Scott, N. R. (2014). Conventional mesophilic vs. thermophilic anaerobic digestion: a trade-off between performance and stability? *Water Research*, *53*, 249–58. https://doi.org/10.1016/j.watres.2014.01.035

Nazari, L., Yuan, Z., Santoro, D., Sarathy, S., Ho, D., Batstone, D., … Ray, M. B. (2017). Low-temperature thermal pre-treatment of municipal wastewater sludge : Process optimization and effects on solubilization and anaerobic degradation. *Water Research*, *113*, 111–123. https://doi.org/10.1016/j.watres.2016.11.055

Noike, T., Endo, G., Chang, J. -E, Yaguchi, J. -I, & Matsumoto, J. -I. (1985). Characteristics of carbohydrate degradation and the rate-limiting step in anaerobic digestion. *Biotechnology and Bioengineering*, *27*(10), 1482–1489. https://doi.org/10.1002/bit.260271013

Rosen, C., & Jeppsson, U. (2006). Aspects on ADM1 Implementation within the BSM2 Framework. *Technical Report*, 1–37.

Souza, T. S. O., Carvajal, A., Donoso-Bravo, A., Peña, M., & Fdz-Polanco, F. (2013). ADM1 calibration using BMP tests for modeling the effect ofautohydrolysis pretreatment on the performance ofcontinuous sludge digesters. *Water Research*, *47*(9), 3244–3254. https://doi.org/10.1016/j.watres.2013.03.041

Tenney, M. W., & Stumm, W. (1965). Chemical flocculation of microorganisms in biological waste treatment. *Journal - Water Pollution Control Federation*, *37*(10), 1370–1388. https://doi.org/10.2307/25035388

Toreci, I., Kennedy, K. J., & Droste, R. L. (2009). Evaluation of continuous mesophilic anaerobic sludge digestion after high temperature microwave pretreatment. *Water Research*, *43*(5), 1273–1284. https://doi.org/10.1016/j.watres.2008.12.022

Vavilin, V. A., Rytov, S. V., & Lokshina, L. Y. (1996). A description of hydrolysis kinetics in anaerobic degradation of particulate organic matter. *Bioresource Technology*, *56*(2–3), 229–237. https://doi.org/10.1016/0960-8524(96)00034-X

3 Temperature impact on solubilization of waste activated sludge in an autohydrolysis pretreatment process

3.1 Introduction

Municipal wastewater treatment plants use anaerobic digesters to stabilize sludge that is produced by the conventional wastewater treatment process. Anaerobic digestion (AD) is a biological process that uses microorganisms to reduce organics into methane gas (Grady et al., 2011). Over the past few years, there is a growing social, economical, and environmental incentive to improve AD. Improving the AD processes allows for a shorter overall digestion process, reducing operating costs and increasing digester capacity. Organics not reduced during the AD process are landfilled, where they breakdown into greenhouse gases (GHG). Stringent regulations on green house gas emissions and landfilling of biosolids from municipal wastewater treatment facilities have made it difficult and expensive for wastewater treatment facilities to dispose of biosolids (Langlois, 2017). Further, increasing the extent of organics reduction would reduce disposal fees and GHG production in landfill sites.

Hydrolysis of particulate organics by extracellular enzymes is the rate limiting reaction in AD (Hélène Carrère et al., 2008). Sludge pretreatment processes are used to increase the rate and extent of digestion. Among the various pretreatment process studied, thermal processes have an advantage in their ability to eliminate biosolid pathogens. Digesters operating at mesophilic temperatures (37℃), rely on surface disposal of biosolids

generated at the end of the AD process, as the high pathogen levels prevent other disposal options. Exceptional quality biosolids have no restrictions on their final disposal and can be used to condition soil or as fertilizer for crops. The United States Environmental Protection Agency (EPA) describes exceptional quality biosolids as having a virtual absence of pathogens (Class A) and a reduced quantity of organics that can attract vectors (Walker, Knight, & Stein, 1994). The EPA provides a time-temperature relationship for producing class A biosolids, with the time condition being under absolute retention of sludge (batch digestion). Thermal pretreatment processes can be used with anaerobic digesters, to improve the rate of digestion, and produce exceptional quality biosolids. This would eliminate the need to landfill biosolids, which ultimately reduces costs for the wastewater treatment facility, decreases GHG emissions, and provides benefits for the neighbouring community.

High-temperature treatment, also known as thermal hydrolysis, describes processes that operate at temperatures greater than 100℃. These processes are extensively studied and are effective at increasing the rate and extent of sludge solubilization. Through these thermal treatment processes, the sludge is physically broken down. Studies have shown that the extent of solubilization increases linearly with temperature, and is independent of sludge source (Hélène Carrère et al., 2008). Greater solubilization is achieved by thermal hydrolysis; however, the process demands a great amount of energy. Low-temperature thermal processes operate at temperatures below 100℃. At low-temperatures, the extent and rate of solubilization are impacted by several factors including, sludge source, temperature, and process time (Pesante & Vidal, 2016).

Low-temperature thermal pretreatment processes are less energy demanding and are safer to operate. Autohydrolysis is a biological pretreatment process that works best at thermophilic temperatures > 42℃. In this process, hydrolytic enzymes are released by active microorganisms found in WAS, when the WAS is deprived of oxygen and is subject to high temperatures (Climent et al., 2007) (Yan, Miyanaga, Xing, & Tanji, 2008). These enzymes assist in breaking down particulate organics, and the extracellular polymeric network. This biological process is also referred to in other studies as the enzymatic hydrolysis or the auto-hydrolytic process, as it uses the WAS hydrolytic potential. A limited number of studies have investigated the autohydrolysis process (Pesante & Vidal, 2016). Carvajal evaluated the pretreatment process examining its impact on subsequent AD and solubilization after 12 hours and 24 hours of treatment at 55 ℃ (Carvajal et al., 2013). In the study, a maximum solubilization of 39% of the total COD was measured after 12 hours of pretreatment (Carvajal et al., 2013). Moreover, full-scale pretreatment using the auto-hydrolytic process has been successfully demonstrated by Monsal, in which a series of digesters hydrolyze the sludge prior to AD.

The objective of this study is to evaluate the impact of temperature and time on the effectiveness of the autohydrolysis pretreatment process in WAS hydrolysis. Treatment times less than 12 hours were examined since the previous study reported a higher hydrolysis rate within the first 12 hours. Additionally, the impact of temperature at 55℃, 65℃ and 75℃ on the rate of hydrolysis was examined.

3.2 Methods and analysis

3.2.1 Reactor construction and operation

Three lab-scale anaerobic digesters with a working volume of 200-mL were built using 250-mL glass bottles. Digesters R1, R2, and R3 were operated at thermophilic temperatures of 55℃, 65℃, and 75℃ respectively. Incubators were used for temperature control. The total sludge retention time (SRT) in the batch digesters was four days, and the digester was sampled at 2 hours, 5 hours, 1 day, 2 days, and 4 days. Biogas was collected using a gas collection bag (2 L capacity, Cali-5 Bond, Calibrated Instruments Inc, NY), to measure gas volume and composition.

The reactor was fed thickened waste activated sludge (TWAS) from a local wastewater treatment facility in Hamilton, Ontario. In the lab, TWAS was stored for a period of less then four days at 4℃ prior to use. The characteristics of the sludge collected varied between the two experiments (Table 3.1). With a working volume of 200-mL, the digester was fed 190-mL of thickened WAS and 10-mL of inoculum from a lab-scale inoculum reactor, which was operated for 8 months at a temperature of 55℃ and a sludge retention time (SRT) of 20 days. The inoculum reactor was fed with the same thickened sludge as the one used for the test digester, operated under continuous batch mode. The TWAS was warmed up to a temperature of 55℃ over two hours prior to starting the experiment. This was done to avoid a thermal shock to the inoculum used. The digester was purged with inert nitrogen gas and the gas bags were initially filled with 60 mL of nitrogen gas, to avoid a vacuum within the digester when sampling.

Table 3.1: Characteristics of TWAS, warmed to a temperature of 55℃ over two hours prior to pretreatment.

Sludge	I	II
TCOD (g/L)	42.5	48.3
SCOD (g/L)	4.3	5.7
TSS (g/L)	38.1	37.5
VSS (g/L)	27.7	29.0
VSS-505 (g/L)	4.4	5.2
VSS-350 (g/L)	17.9	18.7
VSS-205 (g/L)	5.4	5.1
pH	7.30	6.85

3.2.2 Analytical methods

Analysis included measuring the total solids (TS), volatile solids (VS), total COD (TCOD) and soluble COD (SCOD) according to the standard methods (APHA/AWWA/WEF, 2012). The SCOD was measured after filtering a 2-ml sample using a 1.5 μm filter paper (934-AH Glass Microfiber Filters, GE Healthcare Biosciences) and diluting the sample by a factor of 12. The sludge pH (SevenMulti, Mettler Toledo) was also measured throughout the four days and was found to be neutral (6.8 to 7.9). The biogas collected was analysed for CH_4, CO_2, and N_2 using a thermal conductivity detector-gas chromatograph (TCD-GC) (SRI 8610C, SRI Instruments, USA). The TCD-GC used a RESTEK packed column (Restek Corporation, PA) and helium as the carrier gas to separate out the gases. The biogas volume was measured using a water displacement method.

Model variables were measured throughout the experiment by modifying the standard suspended solids analysis method. Volatile suspended solids (VSS) were divided into three fractions: X_{505}, X_{350}, and X_{205}, representing the solids that volatilize at temperatures of 505℃, 350℃, and 205℃ respectively. The volatile fractions were

measured by filtering a diluted 2-mL sample of TWAS using a 1.5 μm filter. The filters were then dried over night and sequentially volatilized at each of the three temperatures to determine the various volatile fractions. The analysis was carried out in duplicates for each sample analysed.

3.2.3 Measuring solubilization

Nazari et al. suggest two equations for calculating solubilization of WAS; Equation 1 for calculating COD solubilization and Equation 2 for calculating VSS solubilization (Nazari et al., 2017). COD solubilization is calculated using the $SCOD_t$ at time (t), initial $SCOD_o$ and the initial $TCOD_o$ (Nazari et al., 2017). Likewise, VSS solubilization is calculated using the VSS_t at time (t), initial VSS_o and the initial TSS_o. The COD solubilization represents the percentage of total COD that is solubilized during the pretreatment processes at time (t) and is a measure of the increase in SCOD. While the VSS solubilization is a measure of the decrease in VSS, as a percentage of the total solids initially.

$$\text{COD solubilization} = \frac{SCOD_t - SCOD_o}{TCOD_o} \times 100 \quad (1)$$

$$\text{VSS solubilization} = \frac{VSS_o - VSS_t}{TSS_o} \times 100 \quad (2)$$

3.3 Results and Discussion

3.3.1 Total chemical oxygen demand

TCOD remained unchanged over the four days of pretreatment (Figure 3.1). Regression analysis on the data shows that a value of zero is within the upper and lower 95 % confidence interval for the slope of the lines representing the change in TCOD over the four days. Thus, any change in TCOD over the four days is insignificant. Pretreatment

processes are not expected to digest the sludge but solubilize it. Significant TCOD reduction at the pretreatment stage is undesirable as it reduces the methane potential of the sludge in the AD stage. The small noise in the data can be attributed to the analysis method, which requires a high dilution of the sludge. Small errors are magnified by a high sludge dilution; thus, given the overall trend of the data, it can be said that the TCOD remained constant for over the pretreatment process.

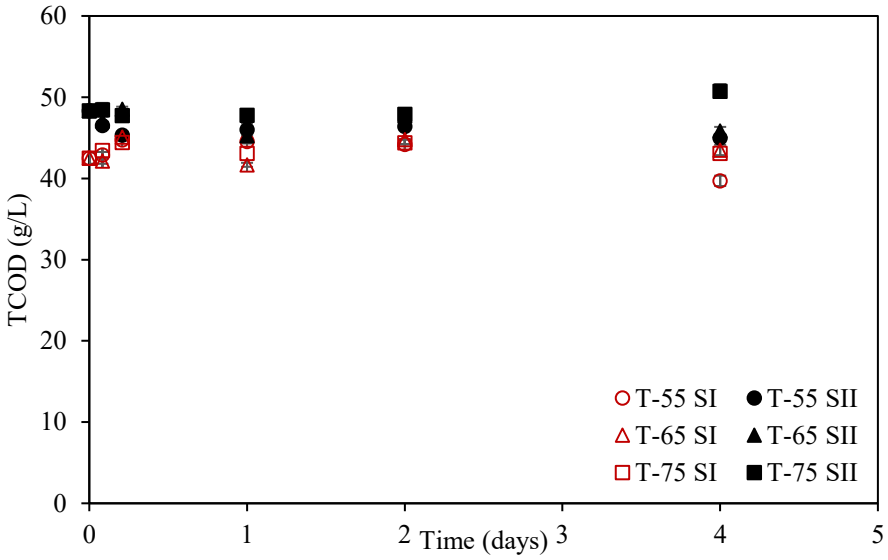

Figure 3.1: TCOD for sludge I (SI) and sludge II (SII), pretreated at three temperatures, 55℃, 65℃ and 75℃ over four days. The error bars represent the standard deviation of the data (n = 2).

3.3.2 Soluble chemical oxygen demand

SCOD typically makes up less than 1% of the TCOD in WAS. SCOD leaving the clarifier in the underflow is the same as that leaving in the overflow. The concentration of the overflow is regulated and must be kept low; thus, the concentration of SCOD in the WAS is also low. Sludge one (SI) had a significantly higher SCOD concentration than sludge two

(SII), 12 % and 10 % respectively (Table 3.1). The two reasons for the higher SCOD measured include a larger filter pore size and sludge warming at 55℃, for two hours prior to characterization. Carvajal et al. define the SCOD as the fraction of organics that can not be filtered, using a filter with a pore size of 0.45µm, and reported a WAS SCOD concentration of 1 % of the TCOD (Carvajal et al., 2013). In this study the SCOD represents the fraction of organics that can not be filtered using a filter with a pore size of 1.5 µm. Thus, organics great in quantity and larger in size were included in the SCOD of this study, that resulted in a higher SCOD value. Additionally, warming the sludge for two hours prior to characterization would have lead to some of the particulate organics breaking down which also contributes to a higher SCOD.

SCOD increased in all three digesters for both SI and SII (Figure 3.2). COD solubilization was more significant in SII; the difference in solubilization between SI and SII can be attributed to differences in sludge properties. Thus, the sludge in SII is more biodegradable. Several factors contribute to the increase in solubilization, including the stimulation of microorganisms, thermal disruption of cells and hydrolysis by anaerobic fermenters. WAS is mainly composed of heterotrophic microorganisms, which when stimulated release enzymes that help breakdown the polymeric network.

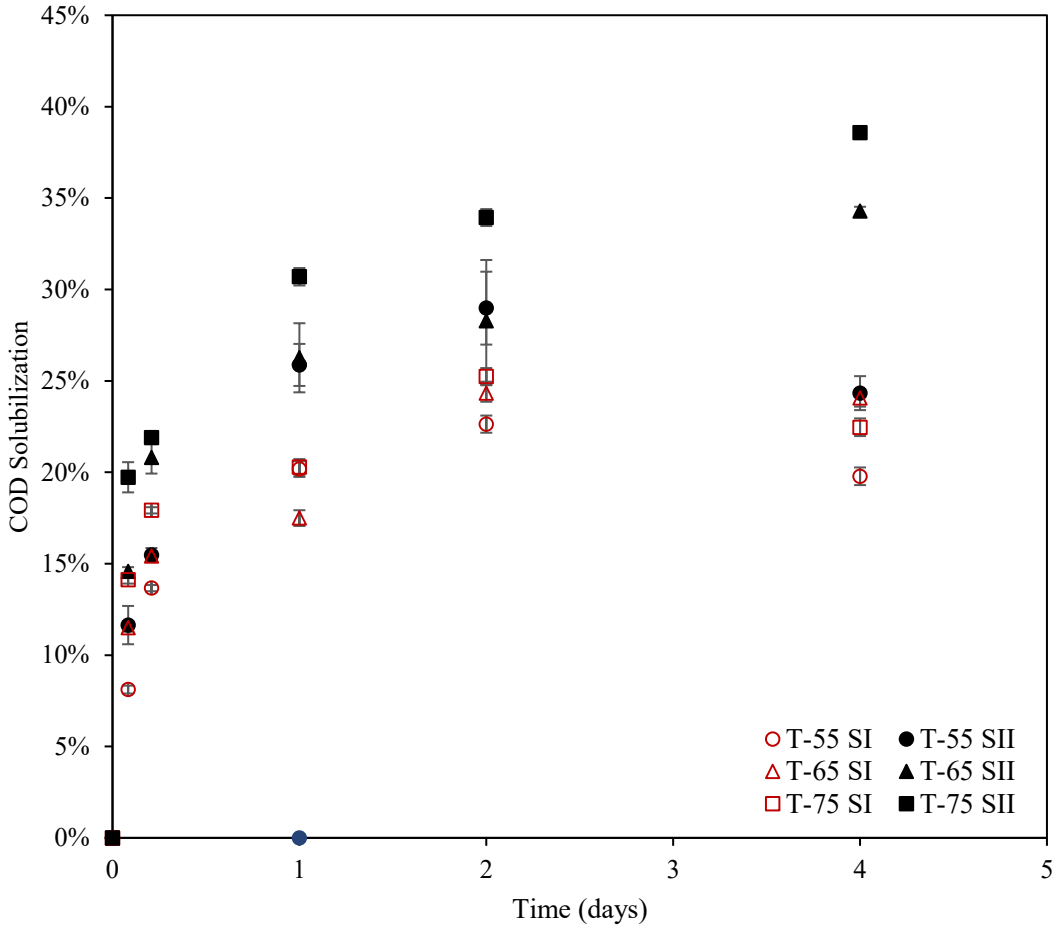

Figure 3.2: COD solubilization of WAS, calculated using Equation 1; for sludge I (SI) and sludge II (SII), pretreated at three temperatures, 55℃, 65℃ and 75℃ over four days. The error bars denote the standard deviation of the data (n = 2).

COD solubilization increased with both factors examined: temperature and time. The shape of the COD solubilization plot resembles the plot generated by the Monod equation. The Monod equation describes the microbial growth rate over a concentration range, whereas Figure 3.2 describes the COD solubilization over time. The Monod plot is characterized by several values including the maximum specific growth rate value, and the half-saturation coefficient. The change in the rate of growth is fastest at a concentration

lower than the half-saturation coefficient and begins to decrease beyond that concentration. The curves in Figure 3.2 also reaches a maximum value and level off. Reaching a maximum value suggests that there is a limit to the solubilization of the TWAS. The "half-saturation" coefficient in Figure 3.2, would be the five-hour retention time. Before the five-hour point, hydrolysis is rapid and increases linearly. After five hours, the rate of hydrolysis decreases and approaches zero as the COD solubilization reaches a maximum. This suggests that the impact of time on hydrolysis decreases over time.

R3 operated at 75℃ had the largest COD solubilization followed by R2 operated at 65℃, indicating that higher temperatures resulted in greater solubilization. In the experiment using SI, the data points cluster up after one day; thus, the impact of temperature becomes less important over time (Figure 3.2). The gap between the three pretreatment temperatures is greatest within the first two hours of pretreatment, meaning that temperature impact was more significant within the first few hours of pretreatment. SI shows a slight decrease in the COD solubilization from day 2 to day 4; Carvajal made a similar observation when conducting a study on solubilization using autohydrolysis, and attributed the reduction in SCOD to consumption by anaerobic microorganisms (Carvajal et al., 2013). However, the decrease in COD solubilization was not consistent between SI and SII, as COD solubilization continues to increase over the four days in the experiment using SII. In this study a COD solubilization high of 38.5 % was achieved at a temperature of 75 ℃ and an SRT of 4 days. Nazari et al. reported similar COD solubilization values. At a temperature of 60℃, neutral pH and an SRT of five hours their pretreatment process reported a COD solubilization of 15.37 % (Nazari et al., 2017). In this study, the average

COD solubilization at 65℃ and five hours of pretreatment was 18.1 % (± 2.69 %). The results suggest that the pretreatment is comparable to other studies. The greater solubilization achieved in this study could be attributed to operating at higher temperatures (+5℃), as well as using a larger pore size filter.

The objectives in a lab are to maximize COD solubilization; however, in an industrial application there are multiple objectives including the reduction of digester SRT, increasing biogas production rate and increasing digester capacity. Pretreatment at 75℃ for a period of four days would provide the maximum COD solubilization; yet, this would increase the SRT of the overall sludge management process. A long SRT would also require larger pretreatment digesters and a greater energy demand. EPA regulations require absolute retention of solids; thus, a digester operated in batch mode is necessary. Given the large volumes of WAS generated, a digester operated in batch mode must have a short SRT, otherwise it would be too large. For industrial application, a shorter SRT is preferred. At a short SRT, the digester is smaller, and thus heating to a temperature of 75℃ is more reasonable. At two hours, the average solubilizations are 9.9 % (±1.8 %), 13.0 % (±1.5 %) and 16.9 % (2.8 %) for reactors R1-55℃, R2-65℃ and R3-75℃ respectively. Based on these results, pretreatment for two hours at a temperature of 75 ℃ is recommended for industrial application. The short pretreatment process will reduce the overall SRT of the sludge management process. Additionally, the pretreatment will satisfy the EPA temperature-time plot requirement for thermally treated biosolids. At 75℃ the temperature-time requirement is only 3 minutes; thus, the biosolids generated at the end of the process can be classified as class A biosolids. Pretreatment at 75℃ for 2 hours increases the rate of

digestion and allows the unregulated use of the biosolids generated. This reduces the disposal costs to the wastewater treatment facility, has a good environmental impact, and provides a benefit to the neighboring community.

3.3.3 Volatile suspended solids

VSS solubilization increase continuously over the four days of pretreatment (Figure 3.3). Different from the COD solubilization plot that levels off after two days of pretreatment, the VSS solubilization plot continues to increase over the four days suggesting the impact of time on solubilization is significant over the four days. The SCOD and the VSS are measurements separated based on size. An increase in the VSS solubilization should also result in an increase in the COD solubilization. The leveling-off of the COD solubilization after two days, is not consistent between the two plots. This means that the SCOD is being used up at a rate equal to the rate at which it is generated. At longer retention times, anaerobic microorganisms begin using the SCOD as substrate. Another explanation is adsorption of the dissolved organics to the particulate organics. Soluble organics that attach to particulate organics are filtered out, resulting in an under representation of the actual SCOD. When the TSS is measured, the soluble organics are volatilized and lost at a temperature of 105℃. The VSS measurement would not include the attached soluble organics and the real reduction in VSS is measured.

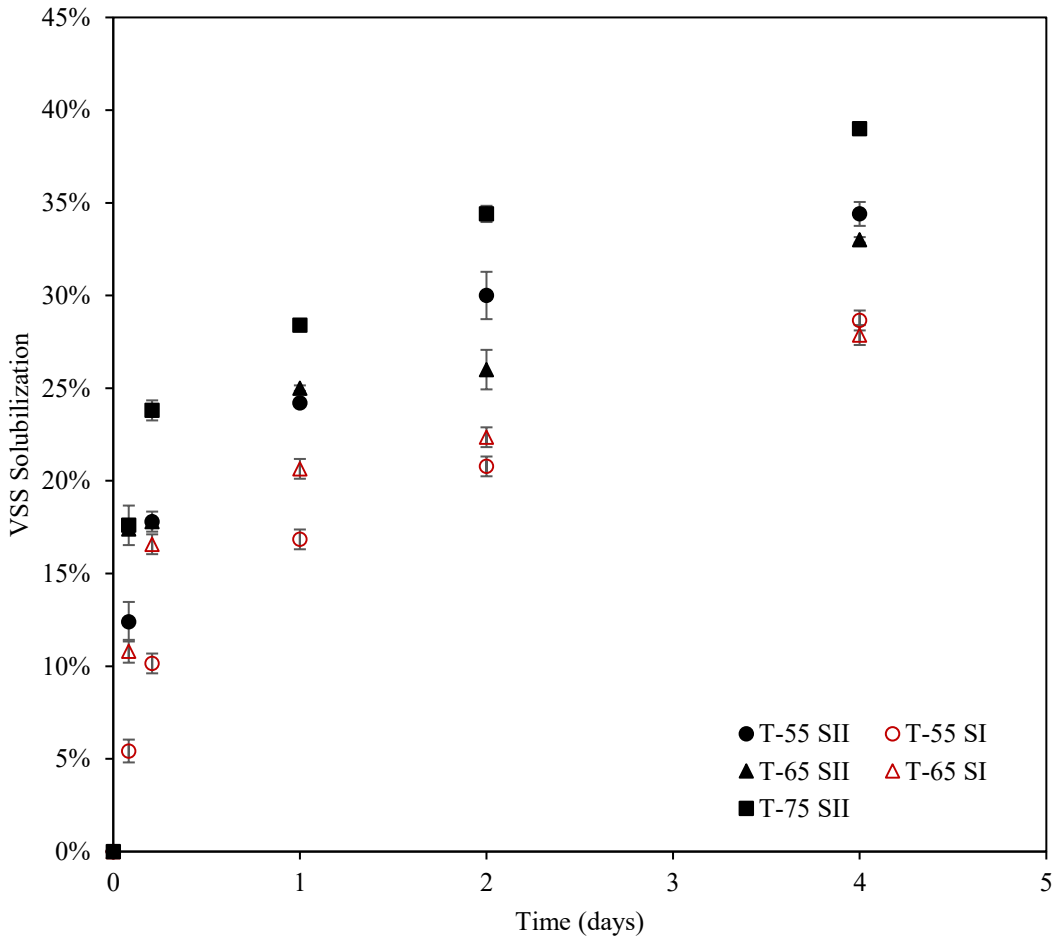

Figure 3.3: VSS solubilization of WAS, calculated using Equation 2; for sludge I (SI) and sludge II (SII), pretreated at three temperatures, 55℃, 65℃ and 75℃ over four days. The error bars denote the standard deviation of the data (n = 2).

Higher VSS solubilization was achieved at higher temperatures, except at 75 ℃ using SI, which were omitted as they were not consistent with what was expected from the results and the trend that the rest of the data follows. Temperature impact on VSS solubilization was more significant at the shorter SRT (Figure 3.3). A maximum 39 % VSS solubilization was achieved in R3-75℃ at four days, half of which was achieved within the first two hours. The VSS reduction results also support the choice for using shorter time

pretreatment processes at higher temperatures. The VSS solubilization at 65℃ after two hours of pretreatment was equal to that at 75℃ in the experiment using SII. This result would suggest pretreating at a temperature of 65℃ for two hours, as the energy demand is less, and the process would still produce class A biosolids. However, more experiments are necessary to compare the VSS solubilization at two hours between R2-65℃ and R3-75℃, since the R3 results of SI are not reliable.

3.3.4 Volatile suspended solids fractions

In the second chapter of this thesis it was determined that the low volatile suspended solids fraction rapidly decreased to a minimum value within the five hours and leveled off for the remainder of the experiment. Similar observations were made in this study, with increased temperatures only impacting the extent of hydrolysis over the first day (Figure 3.4). The increased hydrolysis with temperature increase is expected, as this fraction represents the least volatile suspended solids, which according to the HDM model discussed in the second chapter of this thesis, are not generated from any reaction. On average, 75 % of the degradation measured over the first day occurred within the first two hours of pretreatment, regardless of temperature. These results suggest that pretreatment times of greater than two hours only slightly benefit the degradation of X_{505}, while higher temperatures have a greater impact in the first two hours.

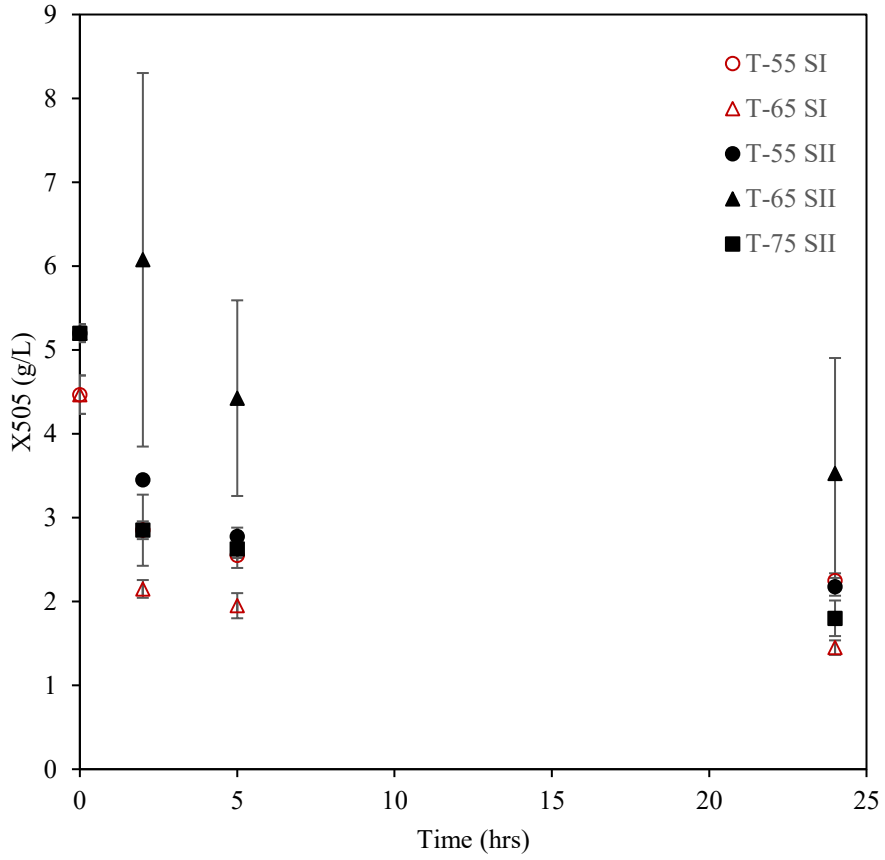

Figure 3.4: Low volatile suspended solids fraction X_{505} of WAS pretreated at three temperatures, 55℃, 65℃ and 75℃ over 24 hours, for sludge I (SI) and sludge II (SII). The error bars denote the standard deviation (n = 2).

X_{350} made up the largest VSS fraction in both experiments and had a similar initial value in both SI and SII (Figure 3.5). X_{350} degraded more rapidly at higher temperatures, in both experiments. The impact of temperature on the extent and rate of degradation was consistent throughout the entire first day. Temperature impact was more significant after five hours of pretreatment. According to HDM, X_{350} is generated by the breakdown of X_{505}. Most of the X_{505} is broken down within the first two hours of pretreatment and to

greater extents at higher temperatures. The rapid generation of the X_{350} from X_{505} within the first two hours of pretreatment results in a reduced temperature impact on the degradation of the X_{350} within the first two hours. After two hours, most of the X_{505} is broken down; thus, X_{350} generation is reduced after two hours.

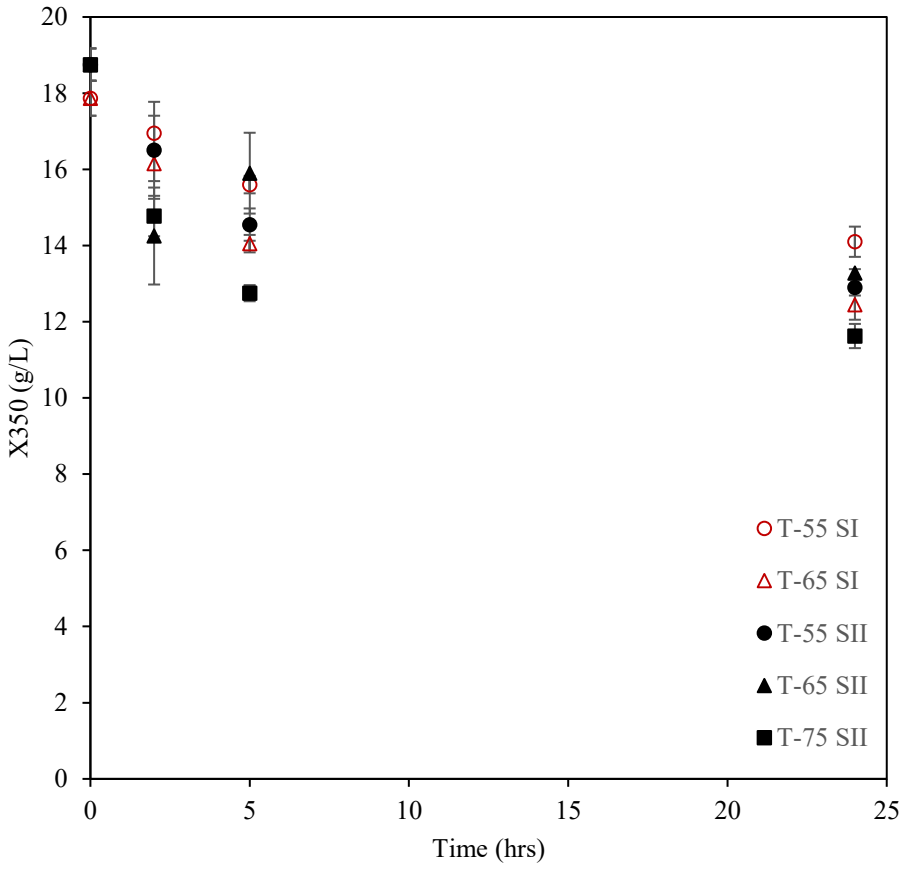

Figure 3.5: Moderately volatile suspended solids fraction X_{350} of WAS pretreated at three temperatures, 55℃, 65℃ and 75℃ over 24 hours, for sludge I (SI) and sludge II (SII). The error bars in the plot denote the standard deviation (n = 2).

X_{205} is constant over the first day of pretreatment and does not appear to be impacted by temperature (Figure 3.6). This was confirmed using statistical analysis, that shows that a value of zero for the slope is within the upper and lower 95 % confidence

interval. This was the case for all the reactors except for R2-65℃ in SII. X_{205} is the most volatile suspended solids fraction and is assumed to be the most biodegradable. The objective of pretreatment processes is to increase the hydrolysis rate, which is often limited by less biodegradable organics, like X_{505} and X_{350}. In HDM, X_{205} is generated by the degradation of X_{350}which degrades at a higher rate at higher pretreatment temperatures. Thus, an accumulation of the X_{205} is to be expected. However, since no significant change in X_{205} was measured within the first day, it can be concluded that the rate of hydrolysis for the two fractions becomes similar.

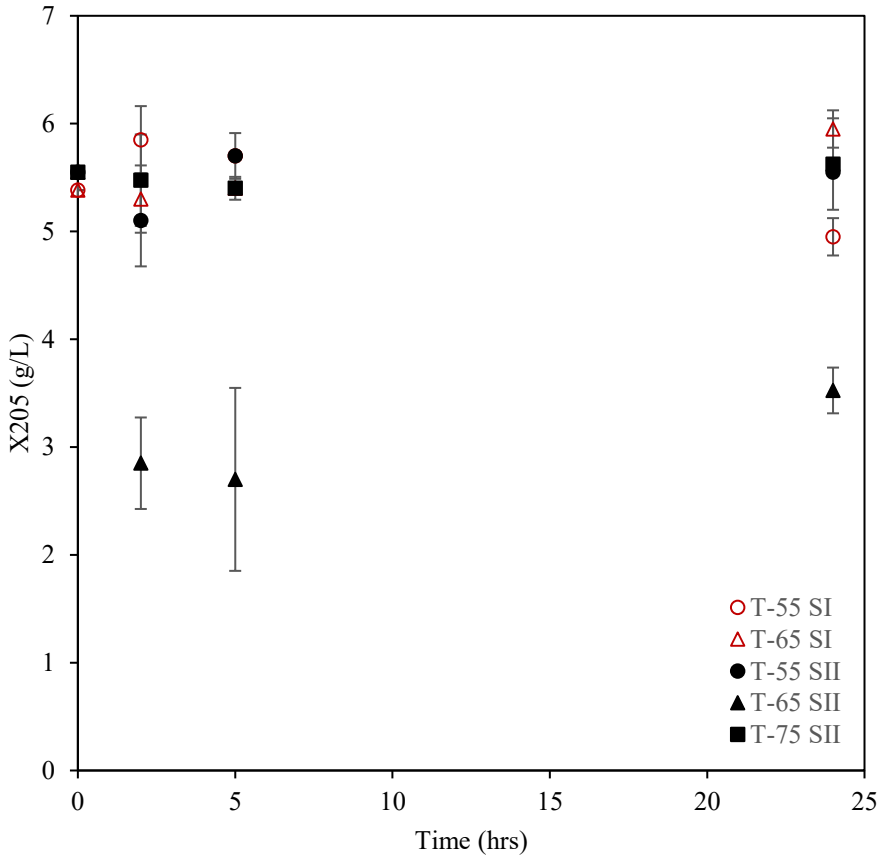

Figure 3.6: High volatile suspended solids fraction X_{205} of WAS pretreated at three temperatures, 55℃, 65℃ and 75℃ over 24 hours, for sludge I (SI) and sludge II (SII). The error bars of the plot denote the standard deviation (n = 2).

3.4 Conclusions

The impact of time and temperature on effectives of the autohydrolysis pretreatment process was examined. Solubilization increased with both temperature and time. Maximum COD and VSS solubilization values of 38.5% and 39% respectively, were measure after four days of pretreatment at a temperature of 75℃. It was also determined that more than 50% of the maximum solubilization values measured after four days of pretreatment were achieved within the first two hours of pretreatment. The high rate of solubilization within the first two hours of pretreatment has potential for industrial application, as treatment for two hours at 75℃ guarantees the generation of class A biosolids. It is recommended that more repetitions of the experiment be completed, as some of the data was omitted in this study.

3.5 References

APHA/AWWA/WEF. (2012). Standard Methods for the Examination of Water and Wastewater. *Standard Methods*, 541. https://doi.org/ISBN 9780875532356

Carrère, H., Bougrier, C., Castets, D., & Delgenès, J. P. (2008). Impact of initial biodegradability on sludge anaerobic digestion enhancement by thermal pretreatment. *Journal of Environmental Science and Health - Part A Toxic/Hazardous Substances and Environmental Engineering*, *43*(13 SPEC. ISS.), 1551–1555. https://doi.org/10.1080/10934520802293735

Carvajal, A., Peña, M., & Pérez-Elvira, S. (2013). Autohydrolysis pretreatment of secondary sludge for anaerobic digestion. *Biochemical Engineering Journal*, *75*, 21–31. https://doi.org/10.1016/j.bej.2013.03.002

Climent, M., Ferrer, I., Baeza, M. del M., Artola, A., Vázquez, F., & Font, X. (2007). Effects of thermal and mechanical pretreatments of secondary sludge on biogas production under thermophilic conditions. *Chemical Engineering Journal*, *133*(1–3), 335–342. https://doi.org/10.1016/j.cej.2007.02.020

Grady, C. P. L. G., Daigger, G. T., Love, N. G., & Filipe, C. D. M. (2011). *Biological Wastewater Treatment, Third Edition* (3, revised ed.). IWA Publishing. Retrieved from https://books.google.ca/books?id=stjLBQAAQBAJ&dq=biological+methods+of+wastewater+treatment+third+edition&lr=&source=gbs_navlinks_s

Langlois, S., & Director, -Blouin. (2017). Quebec's Organics Disposal Ban Strategy Webinar – NZWC Food Working Group. Retrieved from http://www.nzwc.ca/webinars/Documents/SophieLanglois-Blouin_Webinar_Dec-7-2017-v3f.pdf

Nazari, L., Yuan, Z., Santoro, D., Sarathy, S., Ho, D., Batstone, D., … Ray, M. B. (2017). Low-temperature thermal pre-treatment of municipal wastewater sludge : Process optimization and effects on solubilization and anaerobic degradation. *Water Research*, *113*, 111–123. https://doi.org/10.1016/j.watres.2016.11.055

Pesante, P. N. S., & Vidal, M. V. G. (2016). Developments in pre-treatment methods to improve anaerobic digestion of sewage sludge. *Reviews in Environmental Science and Bio/Technology*, *15*(2), 173–211. https://doi.org/10.1007/s11157-016-9396-8

Walker, J., Knight, L., & Stein, L. (1994). A Plain English Guide to the EPA Part 503 Biosolids Rule, (September), 183. Retrieved from water.epa.gov/scitech/wastetech/biosolids/503pe_index.cfm

Yan, S., Miyanaga, K., Xing, X. H., & Tanji, Y. (2008). Succession of bacterial community and enzymatic activities of activated sludge by heat-treatment for reduction of excess sludge. *Biochemical Engineering Journal*, *39*(3), 598–603.

4 Conclusions

4.1 Hydrolysis digestion model (HDM)

The mathematical model simulations were consistent with both experimental results and existing AD models. The model accurately simulated the sludge hydrolysis and SCOD generation from the experiments. At the same time the model produced a similar methane curve to that of ADM1. The first result shows the model's ability to accurately model hydrolysis reactions, while the second result shows that the model can predict the methane generation at a similar accuracy as ADM1, using significantly less variables, and process reactions. Additionally, the model input variables X_{505}, X_{350}, and X_{205} can be easily measured. All these factors should encourage application of the model to improve existing digesters, and to evaluate pretreatment processes. Pretreatment at higher temperatures increased both VSS and COD solubilization. The temperature impact was most significant within the first five hours of pretreatment. Hydrolysis reactions were most sensitive to time, at shorter pretreatment times. The objective of sludge pretreatment is to reduce the overall process time; thus, industrial pretreatment processes must have a short retention time. Looking at the sludge solubilization data after two hours of pretreatment, digester operated at 75 ℃ resulted in the greatest solubilization.

4.2 Future studies

There are several opportunities to improve and build on the model that was developed. Future work can include adding a temperature correction factor for the hydrolysis rate constants ($k_{hyd,505}$, $k_{hyd,350}$, $k_{hyd,205}$). Because many of the existing pretreatment processes are temperature dependent, a temperature correction factor would be valuable to modify the model and to use in various applications. To find a temperature correction factor, lab scale experiments like those conducted in chapter 3 of this thesis can be conducted. Model simulations can be fitted to experimental data from the lab scale AD operated at various temperature conditions. A temperature correction factor can be determined using the hydrolysis rate constants from each simulation.

The model developed is a non-steady state model. Most anaerobic digesters and sludge pretreatment processes are operated in a continuous or semi-batch mode. Future studies can pursue investigation using the model to simulate full scale municipal anaerobic digesters or pilot studies. An example of a local pilot study that uses the enzymatic hydrolysis pretreatment processes is Suez's advanced anaerobic digestion process in Guelph, Ontario. To carry this out, the model must be developed in steady-state using Table A1.

Modifying and repeating the experiments in chapter 3 would be useful. Based on the results obtained, sludge hydrolysis is most significant during the first two hours of treatment. To better examine what happens within the first two hour of pretreatment, actions to modify the experiment sampling procedure to 30, 60, 90, 120 minutes and 5

hours would be taken. Results are predicted to demonstrate that the rate of hydrolysis will be even greater within those first two hours. Shorter treatment times are more desirable for industrial applications especially when the digester is operated in batch mode.

Another modification that could be applied to the experiment would be to determine the absolute retention time required to achieve class A biosolids and pre-treat the sludge for that length of time after the digester reaches the desired temperature. For example, at 65℃ the retention time requirement is 1 hour; thus, fresh sludge can be heated until it reaches a temperature of 65℃. After a temperature of 65℃ is attained, it can be held at that temperature for an hour. The experiments can be repeated for several temperatures, and the solubilization examined. This way, all processes would result in Class A biosolids. The total treatment time and the hydrolysis analysis can be used to determine the optimum pretreatment configuration. Additionally, the energy demand of each pretreatment process can be calculated and used as a third factor in determining the optimal pretreatment process.

Appendix A: Model kinetics

Table A0.1: Biochemical kinetic rate equations (j) and the rate coefficients for both soluble and particulate components (i).

Component (i) → **Process (j) ↓**		1	2	3	4	5	6	7	8	9	10	11	12	**Rate (R)**
		S_{Org}	S_{VFA}	S_{H_2}	S_I	S_{CH_4}	X_{505}	X_{350}	X_{205}	X_I	X_F	X_{VFA}	X_{H_2}	
1	Hydrolysis low volatile fraction	$f_{505,S_{Org}}$					-1	$f_{505,350}$						If $X_F < X_F^*$, $R = k_{hyd,505} X_{505} X_F$ If $X_F \geq X_F^*$, $R = k_{hyd,350} X_{505} X_F^*$
2	Hydrolysis moderate volatile fraction	$f_{350,S_{Org}}$						-1	$f_{350,205}$					If $X_F < X_F^*$, $R = k_{hyd,350} X_{350} X_F$ If $X_F \geq X_F^*$, $R = k_{hyd,350} X_{350} X_F^*$
3	Hydrolysis high volatile fraction	$f_{205,S_{Org}}$							-1					If $X_F < X_F^*$, $R = k_{hyd,205} X_{205} X_F$ If $X_F \geq X_F^*$, $R = k_{hyd,205} X_{205} X_F^*$
4	Fermentation of Organics	-1	$\left(1 - Y_{S_{Org}}\right) * f_{S_{Org},S_{VFA}}$	$\left(1 - Y_{S_{Org}}\right) * f_{S_{Org},S_{H_2}}$							$Y_{S_{Org}}$			$k_{org} \frac{S_{Org}}{S_{Org} + K_{s_{Org}}} X_F$
5	VFA Methanogenesis		-1			$(1 - Y_{S_{VFA}})$						$Y_{S_{VFA}}$		$k_{VFA} \frac{S_{VFA}}{S_{VFA} + K_{s_{VFA}}} X_{VFA}$
6	Hydrogenotrophic Methanogenesis			-1		$(1 - Y_{S_{H_2}})$							$Y_{S_{H_2}}$	$k_{h_2} \frac{S_{H_2}}{S_{H_2} + K_{s_{h2}}} X_{H_2}$
7	Decay of Fermenters						$f_{X_F,X_{505}}$			f_{X_F,X_I}	-1			$k_{dec,X_F} X_F$
8	Decay of VFA Methanogens						$f_{X_{VFA},X_{505}}$			f_{X_{VFA},X_I}		-1		$k_{dec,X_{VFA}} X_{VFA}$
9	Decay of Hydrogenotrophic Methanogens						$f_{X_{H_2},X_{505}}$			$f_{X_{H_2},X_I}$			-1	$k_{dec,X_{H_2}} X_{H_2}$
10	Hydrolysis of Particulate Inert				f_{X_I,S_I}					$-f_{X_I,S_I}$				$k_{hyd,X_I} X_I * X_F$

Appendix B: Non-steady state mass balance equations for HDM

Δt is the time step, set in the model as 10 minutes.

(t_i) is the time step i.

B1. Mass balance on soluble organics S_{Org}

If $X_F < X_F^*$

$$S_{Org}(t_i) = \frac{S_{Org}(t_i - 1) + \Delta t * \left(f_{505,S_{org}} * k_{hyd,505} X_{505} X_F + f_{350,S_{org}} * k_{hyd,350} X_{350} X_F + f_{205,S_{org}} * k_{hyd,205} X_{205} X_F\right)}{1 + \Delta t * k_{org} * \frac{1}{S_{Org} + K_{s_{Org}}} * X_F}$$

If $X_F \geq X_F^*$

$$S_{Org}(t_i) = \frac{S_{Org}(t_i - 1) + \Delta t * \left(f_{505,S_{org}} * k_{hyd,505} X_{505} X_F^* + f_{350,S_{org}} * k_{hyd,350} X_{350} X_F^* + f_{205,S_{org}} * k_{hyd,205} X_{205} X_F^*\right)}{1 + \Delta t * k_{org} * \frac{1}{S_{Org} + K_{s_{Org}}} * X_F}$$

B2. Mass balance on soluble volatile fatty acids S_{VFA}

$$S_{VFA}(t_i) = \frac{S_{VFA}(t_i - 1) + \left(\Delta t * \left(1 - Y_{S_{Org}}\right) * f_{S_{Org},S_{VFA}} * k_{org} * \frac{S_{Org}}{S_{Org} + K_{s_{Org}}} * X_F\right)}{1 + \Delta t * k_{VFA} * \frac{1}{S_{VFA} + K_{s_{VFA}}} * X_{VFA}}$$

B3. Mass balance on dissolved hydrogen gas S_{H_2}

$$S_{H_2}(t_i) = \frac{S_{H_2}(t_i - 1) + \Delta t * \left(\left(1 - Y_{S_{Org}}\right) * f_{S_{Org},S_{H_2}} * k_{org} * \frac{S_{Org}}{S_{Org} + K_{s_{Org}}} * X_F\right)}{1 + \Delta t * k_{h_2} * \frac{1}{S_{H_2} + K_{s_{h2}}} * X_{H_2}}$$

B4. Mass balance on soluble inert S_I

If $X_F < X_F^*$

$$S_I(t_i) = S_I(t_i - 1) + \Delta t * f_{XI,SI} * k_{hyd,X_i} X_I * X_F$$

If $X_F \geq X_F^*$

$$S_I(t_i) = S_I(t_i - 1) + \Delta t * f_{XI,SI} * k_{hyd,X_i} X_I * X_F^*$$

B5. Mass balance on methane gas S_{CH4}

$$S_{CH_4}(t_i) = S_{CH_4}(t_i - 1) + \Delta t * \left(\begin{array}{c} \left(1 - Y_{S_{VFA}}\right) * k_{VFA} * \dfrac{S_{VFA}}{S_{VFA} + K_{s_{VFA}}} * X_{VFA} \\ + \left(1 - Y_{S_{H_2}}\right) * k_{h_2} * \dfrac{S_{H_2}}{S_{H_2} + K_{s_{h2}}} * X_{H_2} \end{array} \right)$$

B6. Mass balance on low volatile suspended solids X_{505}

If $X_F < X_F^*$

$$X_{505}(t_i) = \frac{X_{505}(t_i - 1) + \Delta t * \left(\begin{array}{c} f_{X_F,X_{505}} * k_{dec,X_F} X_F + f_{X_{VFA},X_{505}} * k_{dec,X_{VFA}} X_{VFA} \\ + f_{X_{H_2},X_{505}} * k_{dec,X_{H_2}} X_{H_2} \end{array} \right)}{1 + \Delta t * k_{hyd,505} X_F}$$

If $X_F \geq X_F^*$

$$X_{505}(t_i) = \frac{X_{505}(t_i - 1) + \Delta t * \left(\begin{array}{c} f_{X_F,X_{505}} * k_{dec,X_F} X_F + f_{X_{VFA},X_{505}} * k_{dec,X_{VFA}} X_{VFA} \\ + f_{X_{H_2},X_{505}} * k_{dec,X_{H_2}} X_{H_2} \end{array} \right)}{1 + \Delta t * k_{hyd,505} X_F^*}$$

B7. Mass balance on moderately volatile suspended solids X_{350}

If $X_F < X_F^*$

$$X_{350}(t_i) = \frac{X_{350}(t_i - 1) + \Delta t * f_{505,350} * k_{hyd,505} X_{505} X_F}{1 + \Delta t * k_{hyd,350} X_F}$$

If $X_F \geq X_F^*$

$$X_{350}(t_i) = \frac{X_{350}(t_i - 1) + \Delta t * f_{505,350} * k_{hyd,505} X_{505} X_F^*}{1 + \Delta t * k_{hyd,350} X_F^*}$$

B8. Mass balance on high volatile suspended solids X_{205}

If $X_F < X_F^*$

$$X_{205}(t_i) = \frac{X_{205}(t_i - 1) + \Delta t * f_{350,205} * k_{hyd,350} X_{350} X_F}{1 + \Delta t * k_{hyd,205} X_F}$$

If $X_F \geq X_F^*$

$$X_{205}(t_i) = \frac{X_{205}(t_i - 1) + \Delta t * f_{350,205} * k_{hyd,350} X_{350} X_F^*}{1 + \Delta t * k_{hyd,205} X_F^*}$$

B9. Mass balance on inert suspended solids X_I

If $X_F < X_F^*$

$$X_I(t_i) = \frac{X_I(t_i - 1) + \Delta t * \left(f_{X_F,X_I} * k_{dec,X_F} X_F + f_{X_{VFA},X_I} * k_{dec,X_{VFA}} X_{VFA} + f_{X_{H_2},X_I} * k_{dec,X_{H_2}} X_{H_2}\right)}{1 + \Delta t * f_{XI,SI} * k_{hyd,X_i} * X_F}$$

If $X_F \geq X_F^*$

$$X_I(t_i) = \frac{X_I(t_i - 1) + \Delta t * \left(f_{X_F,X_I} * k_{dec,X_F} X_F + f_{X_{VFA},X_I} * k_{dec,X_{VFA}} X_{VFA} + f_{X_{H_2},X_I} * k_{dec,X_{H_2}} X_{H_2}\right)}{1 + \Delta t * f_{XI,SI} * k_{hyd,X_i} * X_F^*}$$

B10. Mass balance on fermenters X_F

$$X_F(t_i) = \frac{X_F(t_i - 1)}{1 + \Delta t * \left(k_{dec,X_F} - Y_{S_{Org}} * k_{org} * \frac{S_{Org}}{S_{Org} + K_{s_{Org}}}\right)}$$

B11. Mass balance on acetoclastic methanogens X_{VFA}

$$X_{VFA}(t_i) = \frac{X_{VFA}(t_i - 1)}{1 + \Delta t * \left(k_{dec,X_{VFA}} - Y_{S_{VFA}} * k_{VFA} * \frac{S_{VFA}}{S_{VFA} + K_{s_{VFA}}}\right)}$$

B12. Mass balance on hydrogenotrophic methanogens X_{H_2}

$$X_{H_2}(t_i) = \frac{X_{H_2}(t_i - 1)}{1 + \Delta t * \left(k_{dec,X_{H_2}} - Y_{S_{H_2}} * k_{h_2} * \frac{S_{H_2}}{S_{H_2} + K_{S_{h2}}}\right)}$$

Appendix C: Non-steady state mass balance equations for ADM1

Δt is the time step, set in the model as 10 minutes.

(t_i) is the time step i.

B1. Mass balance on soluble sugars S_{su}

$$S_{su}(t_i) = \frac{S_{su}(t_{i-1}) + \Delta t * \left(k_{hyd,ch} * X_{Ch} + \left(1 - f_{fa,li}\right) * k_{hyd,li} * X_{Li}\right)}{1 + \Delta t * k_{su} * \frac{1}{K_{S,Su} + S_{su}} * X_{su} * I1(1)}$$

B2. Mass balance on soluble amino acids S_{aa}

$$S_{aa}(t_i) = \frac{S_{aa}(t_{i-1}) + \Delta t * k_{hyd,Pr} * X_{pr}}{1 + \Delta t * k_{aa} * \frac{1}{K_{s,aa} + S_{aa}} * X_{aa} * I1(2)}$$

B3. Mass balance on soluble fatty acids S_{f_a}

$$S_{fa}(t_i) = \frac{S_{fa}(t_{i-1}) + \Delta t * k_{hyd,li} * X_{Li}}{1 + \Delta t * k_{fa} * \frac{1}{K_{s,fa} + S_{fa}} * X_{fa} * I2(1)}$$

B4. Mass balance on soluble valerate S_{va}

$$S_{va}(t_i) = \frac{S_{va}(t_{i-1}) + \Delta t * (1 - Y_{aa}) * f_{va,aa} * k_{aa} * \frac{S_{aa}}{K_{s,aa} + S_{aa}} * X_{aa} * I1(2)}{1 + \Delta t * k_{c4} * \frac{1}{(K_{s,c4} + S_{va})} * X_{c4} * \frac{1}{(S_{va} + S_{bu})} * I2(2)}$$

B5. Mass balance on soluble butyrate S_{bu}

$$S_{bu}(t_i) = \frac{S_{bu}(t_{i-1}) + \Delta t * \left(\begin{array}{c} (1 - Y_{su}) * f_{bu,su} * k_{su} * \frac{S_{su}}{(K_{S,Su} + S_{su})} * X_{su} * I1(1) \\ +(1 - Y_{aa}) * f_{bu,aa} * k_{aa} * \frac{S_{aa}}{K_{s,aa} + S_{aa}} * X_{aa} * I1(2) \end{array} \right)}{1 + \Delta t * k_{c4} * \frac{1}{(K_{s,c4} + S_{bu})} * X_{c4} * \frac{1}{(S_{va} + S_{bu})} * I2(3)}$$

B6. Mass balance on soluble propionate S_{pro}

$$S_{pro}(t_i) = \frac{S_{pro}(t_{i-1}) + \Delta t * \left(\begin{array}{c} (1 - Y_{su}) * f_{pro,su} * k_{su} * \frac{S_{su}}{K_{S,Su} + S_{su}} * X_{su} * I1(1) \\ +(1 - Y_{aa}) * f_{pro,aa} * k_{aa} * \frac{S_{aa}}{(K_{s,aa} + S_{aa})} * X_{aa} * I1(2) \\ + (1 - Y_{c4}) * 0.54 * k_{c4} * \frac{S_{va}}{(K_{s,c4} + S_{va})} * X_{c4} * \frac{S_{va}}{(S_{va} + S_{bu})} * I2(2) \end{array} \right)}{1 + \Delta t * k_{pro} * \frac{1}{K_{s,pro} + S_{pro}} * X_{pro} * I2(4)}$$

B7. Mass balance on soluble acetate S_{ac}

$$S_{ac}(t_i) = \frac{S_{ac}(t_{i-1}) + \Delta t * \left(\begin{array}{c} (1 - Y_{su}) * f_{ac,su} * k_{su} * \frac{S_{su}}{K_{S,Su} + S_{su}} * X_{su} * I1(1) \\ +(1 - Y_{aa}) * f_{ac,aa} * k_{aa} * \frac{S_{aa}}{(K_{s,aa} + S_{aa})} * X_{aa} * I1(2) \\ +(1 - Y_{fa}) * 0.7 * k_{fa} * \frac{S_{fa}}{K_{s,fa} + S_{fa}} * X_{fa} * I2(1) \\ +(1 - Y_{c4}) * 0.31 * k_{c4} * \frac{S_{va}}{(K_{s,c4} + S_{va})} * X_{c4} * \frac{S_{va}}{(S_{va} + S_{bu})} * I2(2) \\ +(1 - Y_{c4}) * 0.8 * k_{c4} * \frac{S_{bu}}{(K_{s,c4} + S_{bu})} * X_{c4} * \frac{S_{bu}}{(S_{va} + S_{bu})} * I2(3) \\ +(1 - Y_{pro}) * 0.57 * k_{pro} * \frac{S_{pro}}{(K_{s,pro} + S_{pro})} * X_{pro} * I2(4) \end{array} \right)}{1 + \Delta t * k_{ac} * \frac{1}{(K_{s,ac} + S_{ac})} * X_{ac} * I3}$$

B8. Mass balance on soluble hydrogen gas S_{h2}

$$S_{h2}(t_i) = \frac{S_{h2}(t_{i-1}) + \Delta t * \begin{pmatrix} (1-Y_{su}) * f_{h2,su} * k_{su} * \frac{S_{su}}{K_{S,Su} + S_{su}} * X_{su} * I1(1) \\ +(1-Y_{aa}) * f_{h2,aa} * k_{aa} * \frac{S_{aa}}{K_{s,aa} + S_{aa}} * X_{aa} * I1(2) \\ +(1-Y_{fa}) * 0.3 * k_{fa} * \frac{S_{fa}}{K_{s,fa} + S_{fa}} * X_{fa} * I2(1) \\ +(1-Y_{c4}) * 0.15 * k_{c4} * \frac{S_{va}}{(K_{s,c4} + S_{va})} * X_{c4} * \frac{S_{va}}{(S_{va} + S_{bu})} * I2(2) \\ +(1-Y_{c4}) * 0.2 * k_{c4} * \frac{S_{bu}}{(K_{s,c4} + S_{bu})} * X_{c4} * \frac{S_{bu}}{(S_{va} + S_{bu})} * I2(3) \\ +(1-Y_{pro}) * 0.43 * k_{pro} * \frac{S_{pro}}{K_{s,pro} + S_{pro}} * X_{pro} * I2(4) \end{pmatrix}}{1 + \Delta t * k_{h2} * \frac{1}{K_{s,h2} + S_{h2}} * X_{h2} * I1(3)}$$

B9. Mass balance on methane gas S_{CH_4}

$$S_{ch4}(t_i) = S_{ch4}(t_{i-1}) + \Delta t * ((1-Yac) * k_{ac} * \frac{S_{ac}}{(K_{s,ac} + S_{ac})} * X_{ac} * I3 + (1-Y_{h2}) * k_{h2} * \frac{S_{h2}}{K_{s,h2} + S_{h2}} * X_{h2} * I1(3))$$

B10. Mass balance on particulate composites X_C

$$X_C(t_i) = \frac{X_C(t_{i-1}) + \Delta t * \begin{pmatrix} k_{dec,xsu} * X_{su} + k_{dec,xaa} * X_{aa} + k_{dec,xfa} * X_{fa} \\ +k_{dec,xc4} * X_{c4} + k_{dec,xpro} * X_{pro} \\ +k_{dec,xac} * X_{ac} + k_{dec,xh2} * X_{h2} \end{pmatrix}}{1 + \Delta t * k_{dis}}$$

B11. Mass balance on particulate carbohydrates X_{ch}

$$X_{ch}(t_i) = \frac{X_{ch}(t_{i-1}) + \Delta t * f_{ch,xc} * k_{dis} * X_C}{1 + \Delta t * k_{hyd,ch}}$$

B12. Mass balance on particulate protein X_{pr}

$$X_{pr}(t_i) = \frac{X_{pr}(t_{i-1}) + \Delta t * f_{pr,xc} * k_{dis} * X_C}{1 + \Delta t * k_{hyd,Pr}}$$

B13. Mass balance on particulate lipids X_{li}

$$X_{Li}(t_i) = \frac{X_{li}(t_{i-1}) + \Delta t * f_{li,xc} * k_{dis} * X_C}{1 + \Delta t * k_{hyd,li}}$$

B14. Mass balance on sugar degraders X_{su}

$$X_{su}(t_i) = \frac{X_{su}(t_{i-1})}{1 - \Delta t * (Y_{su} * k_{su} * \frac{S_{su}}{(K_{S,Su} + S_{su})} * I1(1) - k_{dec,xsu}}$$

B15. Mass balance on amino acid degraders X_{aa}

$$X_{aa}(t_i) = \frac{X_{aa}(t_{i-1})}{1 - \Delta t * (Y_{aa} * k_{aa} * \frac{S_{aa}}{K_{s,aa} + S_{aa}} * I1(2) - k_{dec,xaa}}$$

B16. Mass balance on LCFA degraders X_{fa}

$$X_{fa}(t_i) = \frac{X_{fa(t_{i-1})}}{1 - \Delta t * \left(Y_{fa} * k_{fa} * \frac{S_{fa}}{(K_{s,fa} + S_{fa})} * I2(1) - k_{dec,xfa} \right)}$$

B17. Mass balance on butyrate degraders X_{c4}

$$X_{c4}(t_i) = \frac{X_{c4}(t_{i-1})}{1 - \Delta t * Y_{c4} * \left(\begin{array}{c} k_{c4} * \frac{S_{va}}{(K_{s,c4} + S_{va})} * (S_{va}(S_{va} + S_{bu})) * I2(2) \\ +k_{c4} * \frac{S_{bu}}{(K_{s,c4} + S_{bu})} * (S_{bu}(S_{va} + S_{bu})) * I2(3) \\ -k_{dec,xc4} \end{array} \right)}$$

B18. Mass balance on propionate degraders X_{pro}

$$X_{pro}(t_i) = \frac{X_{pro}(t_{i-1})}{1 - \Delta t * (Y_{pro} * k_{pro} * \frac{S_{pro}}{(K_{s,pro} + S_{pro)}} * I2(4) - k_{dec,xpro})}$$

B19. Mass balance on acetoclastic methanogens X_{ac}

$$X_{ac}(t_i) = \frac{X_{ac}(t_{i-1})}{1 - \Delta t * \left(Y_{ac} * k_{ac} * \frac{S_{ac}}{(K_{s,ac} + S_{ac})} * I3 - k_{dec,xac} \right)}$$

B20. Mass balance on hydrogenotrophic methanogens X_{h2}

$$X_{h2}(t_i) = \frac{X_{h2}(t_{i-1})}{1 - \Delta t * \left(Y_{h2} * k_{h2} * \frac{S_{h2}}{(K_{s,h2} + S_{h2})} * I1(3) - k_{dec,xh2} \right)}$$

B21. Mass balance on particulate Inert solids X_I

$$X_I(t_i) = \left(X_I(t_{i-1}) + \Delta t * f_{i,xc} * k_{dis} * X_C \right)$$

Appendix D: Gas analysis

Table D1: Digester biogas composition in experiments using sludge I and sludge II. Three digesters were used in each experiment, R1, R2, and R3 operated at 55℃, 65℃ and 75℃ respectively. The results show the percentage of gas in the digester that was methane and carbon dioxide at each sample time 0, 2, 5 24, 48 and 96 hrs. The gas bag was initially filled with 60-mL of nitrogen gas; thus, the remaining percentage in each sample is nitrogen gas.

Sludge I						
	R1-55℃		**R2-65℃**		**R3-75℃**	
Time (hrs)	Methane	Carbon Dioxide	Methane	Carbon Dioxide	Methane	Carbon Dioxide
0	0.00%	0.00%	0.00%	0.00%	0.00%	0.00%
2	0.00%	0.81%	0.95%	0.64%	0.00%	1.80%
5	0.12%	3.82%	0.10%	4.31%	0.07%	4.18%
24	4.24%	18.95%	7.05%	25.42%	0.14%	13.75%
48	9.71%	24.98%	12.70%	29.11%	0.00%	27.38%
96	28.21%	27.58%	15.77%	24.92%	3.29%	31.37%
Sludge II						
	R1-55℃		**R2-65℃**		**R3-75℃**	
Time (hrs)	Methane	Carbon Dioxide	Methane	Carbon Dioxide	Methane	Carbon Dioxide
0	0.00%	0.00%	0.00%	0.00%	0.00%	0.00%
2	1.82%	6.69%	1.56%	5.27%	2.45%	10.19%
5	2.10%	13.25%	1.79%	8.81%	2.54%	17.05%
24	9.48%	34.73%	9.74%	39.56%	2.60%	23.61%
48	15.23%	40.74%	16.69%	44.50%	2.39%	33.08%
96	25.36%	38.88%	19.93%	46.24%	1.98%	31.28%

Table D2: Final volume of biogas in the digester after four days of pretreatment in three digesters R1, R2 and R3, in the experiments using sludge I and sludge II. The gasbag was initially filled with 60-mL of nitrogen gas. 60-mL of sludge were removed from the digester during sampling; thus, the volume represents the total volume of biogas generated.

Biogas volume (mL)		
Temperature	Sludge I	Sludge II
R1-55℃	398	402
R2-65℃	277	362
R3-75℃	160	180